Elevated Temperature Effects on Protein Turnover Dynamics in *Arabidopsis thaliana* Seedlings Revealed by 15N-Stable Isotope Labeling and ProteinTurnover Algorithm

Kai-Ting Fan and Yuan Xu *

Posted Date: 13 May 2024

doi: 10.20944/preprints202405.0780.v1

Keywords: 15N-stable isotope labeling; crop resilience; Arabidopsis thaliana; heat stress; protein turnover; proteomics

 doi:10.20944/preprints202405.0780.v1

Article

Elevated Temperature Effects on Protein Turnover Dynamics in *Arabidopsis thaliana* Seedlings Revealed by ^{15}N-Stable Isotope Labeling and *ProteinTurnover* Algorithm

Kai-Ting Fan [1] and Yuan Xu [2,*]

[1] Agricultural Biotechnology Research Center, Academia Sinica, Taipei, Taiwan; kaitingfan@sinica.edu.tw
[2] MSU-DOE Plant Research Laboratory, Michigan State University, East Lansing, MI 48824, USA; xuyuan5@msu.edu
* Correspondence: xuyuan5@msu.edu

Abstract: Global warming poses a threat to plant survival, impacting growth and agricultural yield. Protein turnover, a critical regulatory mechanism balancing protein synthesis and degradation, is crucial for cellular response to environmental changes. We investigated the effects of elevated temperature on proteome dynamics in *Arabidopsis thaliana* seedlings using ^{15}N-stable isotope labeling and ultra-performance liquid chromatography-high resolution mass spectrometry, coupled with the *ProteinTurnover* algorithm. Analyzing different cellular fractions from plants grown under 22°C and 30°C growth conditions, we found significant changes in the turnover rates of 571 proteins, with a median 1.4-fold increase, indicating accelerated protein dynamics under thermal stress. Notably, soluble root fraction proteins exhibited smaller turnover changes, suggesting tissue-specific adaptations. Significant turnover alterations occurred with redox signaling, stress response, protein folding, secondary metabolism, and photorespiration, indicating complex responses enhancing plant thermal resilience. Conversely, proteins involved in carbohydrate metabolism and mitochondrial ATP synthesis showed minimal changes, highlighting their stability. This analysis highlights the intricate balance between proteome stability and adaptability, advancing our understanding of plant responses to heat stress and supporting the development of improved thermotolerant crops.

Keywords: ^{15}N-stable isotope labeling; crop resilience; *Arabidopsis thaliana*; heat stress; protein turnover; proteomics

1. Introduction

Global warming threatens plant immunity, endangering global food supply and ecosystems [1], with predictions suggesting a decline in crop yields by 11-25% by the century's end [2]. In light of this warming trend, the development of crop varieties engineered for enhanced thermotolerance is imperative to safeguard food production [3,4]. Heat stress manifests observable phenotypes at the whole plant level, including suppressed seed germination, inhibited shoot and root growth, fruit discoloration, leaf senescence, and diminished yield [5]. At the cellular level, heat stress induces physical changes such as increased membrane fluidity and protein denaturation, thereby affecting protein synthesis, enzyme activity, and metabolism [6,7]. Interestingly, moderate heat stress, around 28°C, can trigger phenotypes suggesting improved evaporative cooling capacity despite elevated water loss and transpiration rates [8].

Photosynthesis, particularly Photosystem II (PSII), is significantly affected by heat stress, with moderate heat causing PSII photoinhibition [9] while higher temperatures can lead to dissociation or inhibition of the oxygen-evolving complex [10]. Although Rubisco, the enzyme responsible for carbon fixation, is intrinsically thermostable in higher plants, heat stress can inhibit Rubisco activase, thereby impacting carbon assimilation rates [11,12]. Notably, Rubisco activase acts as a major limiting

 doi:10.20944/preprints202405.0780.v1

factor in plant photosynthesis under heat stress, with the introduction of thermostable Rubisco activase variants resulting in enhanced carbon assimilation rates under moderately high temperatures [11].

Plants employ diverse molecular mechanisms to adapt to elevated ambient temperatures [4,13]. Elevated temperatures elevate the concentration of misfolded, unfolded, and aggregated proteins, triggering the transcriptional activation of heat stress-induced genes [14]. Among these genes are various families of heat shock proteins (HSPs), which act as molecular chaperones regulating protein folding and stability [3]. The unfolded protein response (UPR) in plants represents a vital signaling pathway in response to stress, initiating processes including protein translation attenuation, activation of the ER-associated degradation pathway, and induction of endoplasmic reticulum (ER) chaperones [15]. Heat stress not only affects protein stability but also disrupts specific enzyme functions, thereby perturbing metabolism [16]. Additionally, oxidative stress accompanies the heat stress response, resulting in the accumulation of reactive oxygen species (ROS). Coping with ROS accumulation and other oxidative stress injuries represents a significant challenge for organisms experiencing heat stress [17]. ROS production triggers an antioxidant response mediated through a MAPK signal pathway and induction of downstream transcription factors. A key aspect of this response involves the removal of ROS molecules using ROS scavenging enzymes such as ascorbate peroxidase (APX) and catalase (CAT) [14].

In the realm of genomics, researchers have identified thousands of genes that may be differentially regulated at the transcriptional level in response to heat stress in various plant species, including *Arabidopsis* [18], tomato [19], rice [20], barley [21], wheat [22], and maize [23]. However, the steady-state levels of transcripts do not fully reflect the levels of corresponding proteins, as translation serves as a crucial point of regulatory control in the plant heat stress response [24,25]. These studies underscore the inadequacy of solely relying on transcriptional analyses of the heat response in plants.

Despite continuous advancements in liquid chromatography (LC) coupled mass spectrometry (MS) instrumentation over the past two decades, a limited number of studies have explored the effects of stress conditions on protein dynamics or turnover [26]. One close example is documented by Li et al. [27], who utilized ^{15}N-labeling and two-dimensional fluorescence difference gel electrophoresis with LC-MS/MS to measure the protein degradation rates of 84 proteins in *Arabidopsis* suspension cells. They subsequently calculated protein synthesis rates based on degradation rates and changes in protein relative abundance. The study concluded that protein turnover rates are generally correlated with protein function and among protein complex subunits. Using a similar approach, Nelson et al. measured the degradation rate of mitochondrial proteins using *Arabidopsis* cell cultures with ^{15}N-label incorporation at different time points [28]. These studies employed the *Isodist* algorithm [29] to assign the isotopic abundance to natural abundance and labeled peptide mass spectral data to obtain Relative Isotope Abundance (RIA) values for each peptide throughout the time course. However, a limitation of these approaches is the loss of individual peptide contributions to overall protein turnover due to the use of median peptide RIA values for each protein. In order to detect significant changes in protein turnover rates across different treatments, such as stress conditions, the individual contributions of specific peptides to the overall protein turnover may be easily lost due to the use of median peptide RIA values for each protein. This unnecessarily discards potentially important information regarding the inherent heterogeneity of intracellular protein populations.

Advancing to the studies conducted in planta, proteome-scale analysis has been demonstrated in barley leaves. This was achieved through gas chromatography-mass spectrometry analysis of free amino acids and LC-MS analysis of proteins, enabling tracking the enrichment of ^{15}N into the amino acid pools [30]. Another study utilized a $^{13}CO_2$-labeling approach to quantify the synthesis and degradation rates of selected proteins in Arabidopsis adult plants [31]. Similarly, the degradation rates of ~1200 Arabidopsis leaf proteins have been characterized at different growth and development stages, revealing that protein complex membership and specific protein domains can serve as predictors of degradation rate [32]. However, a comprehensive analysis of plant proteome under

 doi:10.20944/preprints202405.0780.v1

stress conditions has been limited, potentially due to challenges in implementing the methodological pipeline from processing MS data to generating the turnover rate calculations.

In this study, we conducted a proteome-wide analysis to monitor changes in protein turnover in *Arabidopsis thaliana* seedling tissues following exposure to elevated temperature (30˚C). This research introduces, to our knowledge, a novel approach aimed at evaluating, for the first time, the dynamic balance of protein synthesis and degradation in response to moderate heat stress in intact plant seedlings. We utilized the publicly accessible algorithm *ProteinTurnover*, enabling us to execute an automated pipeline to measure protein turnover rates through the ^{15}N-metabolic stable isotope labeling approach on a proteomic scale [33]. As demonstrated in a prior study [34], this algorithm, when combined with stable isotope labeling, offers the capability to explore the comprehensive scope of metabolism, encompassing metabolic rates/fluxes and the static pool size of plants. Our study identified hundreds of proteins exhibiting significant changes in turnover rates in response to elevated temperature stress across root or shoot soluble, organellar, and microsomal fractions.

2. Results

The goal of this study was to evaluate the impact of moderate heat treatment on protein turnover rates across various cellular fractions of Arabidopsis seedling shoots and roots at a proteomic scale. To achieve this aim, seedlings were transferred to media containing stable isotope ^{15}N and subjected to heat stress (30°C), while seedlings under control conditions (22°C) were continuously grown on ^{14}N-medium. Root and shoot tissues were collected at different time points (0, 8, 24, 32, and 48 hours) post-transfer and then subjected to differential centrifugation to isolate fractions enriched in organellar, soluble, or microsome-associated proteins for analysis by LC-MS/MS.

2.1. Peptide Identification and Selection Criteria for Protein Turnover Rate Measurements

From the root tissue, 822 and 857 proteins were identified in the enriched soluble fraction from the control and 30˚C groups, respectively. In the enriched organelle fraction, 494 and 377 proteins were identified from the control and 30˚C groups, respectively. Additionally, 1,222 and 1,054 proteins were identified in the enriched microsomal fraction from the control and 30˚C groups, respectively. Thousands of identified peptides were required for the subsequent turnover analysis due to the lower sensitivity inlet used in this study. As indicated in Table S-1, each sample contained between 5,000 to 14,000 peptides, but only 30-50% of them were present in a sufficient number of time points to compute turnover rates. In this dataset, peptides were most frequently excluded because they were not identified in the time 0 dataset.

Applying multiple quantitative quality criteria for the inclusion of each peptide can enhance the quality of the resulting turnover data and accelerate data processing. Peptides with significant standard errors typically represent those with poor spectral fitting, often due to co-eluting contaminants (Figure 1, panel A). Peptides were included in further analysis if they met specific criteria: a visual score for spectral fitting (to the beta-binomial model) greater than 80 out of 100, a standard error in the turnover rate fitting of less than 10, and data points for at least 3 of the time points (including time 0). These criteria were chosen based on empirical visual inspection of peptide turnover fitting plots generated by the algorithm. Additionally, the normal quantile-quantile (Q-Q) plot of peptide $\log_2 k$ was utilized to assess whether the $\log_2 k$ data were normally distributed (Figure 1, panels B and D). Scatter plots of $\log_2 k$ and the standard error of $\log_2 k$ (such as shown in Figure 1, panels A and C) aided in assessing dataset quality. Inspection of Figure 1 panel C also suggests a potential negative linear correlation between $\log_2 k$ and the standard error of $\log_2 k$, at least for this dataset. Nonetheless, only peptides selected using the aforementioned filtering criteria were used for further turnover rate analysis. Once a peptide passed this filter, it was assumed that the turnover rate calculated for each peptide contributed equally to the final protein turnover rate. Therefore, the $\log_2 k$ of all selected peptides was averaged to yield each individual protein turnover rate ($\log_2 k$) for a given experimental condition (control vs. treatment).

 doi:10.20944/preprints202405.0780.v1

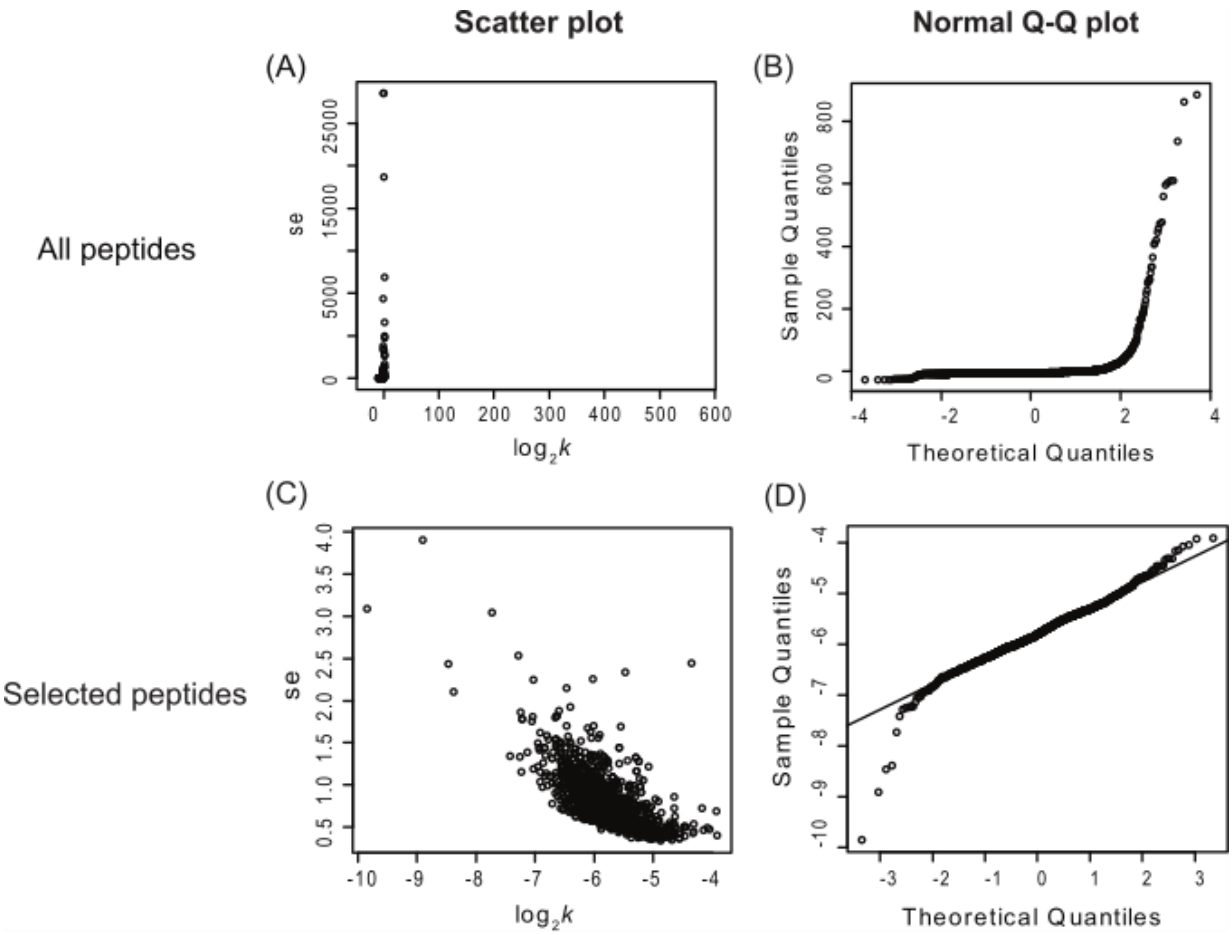

Figure 1. Scatter plots and Normal Q-Q plots of all identified *Arabidopsis* peptides (top) vs. peptides selected with visual scores higher than 80, standard error lower than 10, and at least 3 labeling time points (bottom). The panels on the left (A and C) are scatter plots of the standard error of $\log_2 k$ (se.$\log_2 k$) against $\log_2 k$; the panels on the right (B and D) are normal Q-Q plots of each peptide's turnover rate ($\log_2 k$ values). This figure shows only the peptide data from the enriched shoot soluble fraction and includes data combined from both control and heat treatment groups. The number of peptides is 10,400 (A and B) and 1,273 (C and D). se, standard error.

2.2. Overview of the Effects of Heat Stress on Peptide and Protein Turnover Rates

2.2.1. Trends of Peptide or Protein Turnover Rates

The distributions of peptide turnover rates ($\log_2 k$) between the control and 30˚C groups are depicted for comparison purposes as histograms for soluble, organellar, and microsomal protein-enriched fractions of shoot and root tissues in Figure 2. The distributions of protein turnover rates ($\log_2 k$) between the control and 30˚C groups are illustrated for comparison purposes as histograms for soluble, organellar, and microsomal protein-enriched fractions of shoot and root tissues in Figure 3. When comparing the mean values of peptide turnover rates or the median value of protein turnover rates between roots and shoots, generally across all fractions, the turnover rates of roots were faster than those of shoots. The average protein turnover rate ($\log_2 k$) was -5.308, -5.594, and -5.377 in the soluble, organellar, and microsomal fractions, respectively, while in shoots, the average protein turnover rate was -6.0348, -6.1046, and -5.9765 in the soluble, organellar, and microsomal fractions, respectively. For the control group, the mean protein turnover rates ($\log_2 k$) were close to -5.39 in roots and -6.03 in shoots, indicating that the mean protein half-lives were 29.13 hours in roots and 45.2 hours in shoots, suggesting that root proteome might have a faster turnover rate than shoot proteome in general. This may be related to the development of root tissue in the young seedling

 doi:10.20944/preprints202405.0780.v1

stage of plants, which requires more rapid changes in protein synthesis and degradation. For example, the fast turnover rate of plasma membrane proton pump (ATPase 1) (Table 1) suggests that the establishment of protein machinery for metabolite uptake could be essential for growth at this stage. Although several proteins had dramatically long half-lives (Tables 1 and 2), the average protein turnover rates measured in this study were much faster than the average protein turnover rates in 21 to 26-day-old adult *Arabidopsis* leaves (~4.6 days) as reported in the unpublished work from Millar et al. (presented at the 2015 ASPB conference), suggesting that more rapid protein turnover may be required in the seedling than the adult stage in plants.

Table 1. The 10 fastest and lowest turnover proteins in the enriched soluble or membrane fraction of *Arabidopsis* roots[a].

	ID[b]	Protein	AGI [c]	Fraction[d]	Turnover rate[e]	SD[e]	Functional category[f]
Fastest	Q9M0A7	Putative uncharacterized protein (Gamma-glutamyl peptidase 1)	At4g30530	*S*	-4.397	0.0238	nucleotide met
	A8MRQ4_A8MSB9_F4JTU2_Q9SVM8	Glycine-rich RNA-binding protein 2, mitochondrial	At4g13850	*S*	-4.539	0.1128	RNA
	P20649	ATPase 1, plasma membrane-type	At2g18960	*M*	-4.607	0.0528	transport
	Q9SYM5	Trifunctional UDP-glucose 4,6-dehydratase/UDP-4-keto-6-deoxy-D-glucose 3,5-epimerase/UDP-4-keto-L-rhamnose-reductase RHM1	At1g78570	*M*	-4.624	0.0156	cell wall
	F4KIM7_Q9C5N2	Endomembrane family protein 70	At5g25100	*M*	-4.651	0.0223	N/A
	F4J1V2_Q94AW8	Chaperone protein dnaJ 3	At3g44110	*M*	-4.652	0.0881	stress
	P22953	Probable mediator of RNA polymerase II transcription subunit 37e (Heat Shock cognate Protein 70-1)	At5g02500	*S*	-4.668	0.0276	stress
	Q9XIE2	ABC transporter G family member 36 (AtABCG36)(PEN3)(PDR8)	At1g	*M*	-4.718	0.2347	transport
	P31414	Pyrophosphate-energized vacuolar membrane proton pump 1	At1g15690	*M*	-4.742	0.2033	transport
	Q9S791	Putative uncharacterized protein	At1g70770	*O*	-4.752	0.1353	N/A
Slowest	Q43348	Acid beta-fructofuranosidase 3, vacuolar (Vacuolar invertase 3)	At1g62660	*S*	-6.129	0.3853	major CHO met

 doi:10.20944/preprints202405.0780.v1

Q9C8Y9	Beta-glucosidase 22	At1g66280	*O*	-6.150	0.2910	CHO hydrolases
P43297	Cysteine proteinase RD21a	At1g47128	*M*	-6.170	0.2050	prot.degrad
P25819	Catalase-2	At4g35090	*O*	-6.176	0.4179	redox
Q9FF53	Probable aquaporin PIP2-4 [Cleaved into: Probable aquaporin PIP2-4, N-terminally processed]	At5g60660	*M*	-6.227	0.0228	transport
P46422	Glutathione S-transferase F2	At4g02520	*S*	-6.244	0.0349	GST
A8MR01_F4JR94_O23179	Patatin-like protein 1 (AtPLP1)	At4g37070	*M*	-6.245	0.5113	development
Q9LHB9	Peroxidase 32	At3g32980	*M*	-6.261	0.2944	peroxidases
Q9SIE7	Putative uncharacterized protein (PLAT-plant-stress domain-containing protein)	At2g22170	*S*	-6.314	0.0765	N/A
Q9LTQ5	TRAF-like family protein	At3g20370	*O*	-6.320	0.3226	N/A
Q9C8Y9	Beta-glucosidase 22	At1g66280	*M*	-6.594	0.5007	CHO hydrolases

[a] Complete list in Supplementary Table S-2. Only proteins with at least 2 unique peptides were used to calculate protein turnover rates. [b] Protein accession number assigned by the UniProt database. [c] The gene identification number assigned by the *Arabidopsis* genome initiative. [d] Enriched protein fractions: Microsomal (*M*) fraction from the differential centrifugation (1hr x 100,000 g supernatant) of *Arabidopsis* root or shoot tissue homogenate; Organelle (*O*) fraction from the differential centrifugation (5 min x 1,500 g pellet) of *Arabidopsis* root or shoot tissue homogenate; Soluble (*S*) fraction from the differential centrifugation (1hr x100,000 g pellet) of *Arabidopsis* root or shoot tissue homogenate. [e] Standard deviation of protein turnover rate ($\log_2 k$). [f] The functional category adapted from the MapCave website [62].

Table 2. The 10 fastest and slowest turnover proteins in enriched soluble or membrane fraction of *Arabidopsis* shoots[a].

	ID[b]	Protein	AGI[c]	Fraction[d]	Turnover rate[e]	SD	Functional category[f]
Fastest	B9DG18_Q42547	Catalase-3	At1g20620	*S*	-4.479	0.1605	redox
	Q9CA67	Geranylgeranyl diphosphate reductase, chloroplastic	At1g74470	*M*	-4.746	0.1219	2nd met
	Q9CA67	Geranylgeranyl diphosphate reductase, chloroplastic	At1g74470	*O*	-4.857	0.1659	2nd met
	P56761	Photosystem II D2 protein	AtCg00270	*M*	-4.979	0.1141	PS.light
	P56761	Photosystem II D2 protein	AtCg00270	*O*	-4.986	0.0366	PS.light

 doi:10.20944/preprints202405.0780.v1

	P56778	Photosystem II CP43 reaction center protein	AtCg00280	*M*	-5.101	0.1626	PS.light
	P56778	Photosystem II CP43 reaction center protein	AtCg00280	*O*	-5.127	0.0665	PS.light
	P42761	Glutathione S-transferase F10 (GST class-phi member 10)	At2g30870	*S*	-5.168	0.3743	GST
	Q9LKR3	Mediator of RNA polymerase II transcription subunit 37a (Heat Shock Protein 70-11)	At5g28540	*M*	-5.201	0.4357	stress
	P27202	Photosystem II 10 kDa polypeptide, chloroplastic	At1g79040	*M*	-5.220	0.2322	PS.light
	Q9LJG3	GDSL esterase/lipase ESM1	At3g14210	*O*	-5.261	0.0880	2nd met
	O80860	ATP-dependent zinc metalloprotease FTSH 2, chloroplastic	At2g30950	*O*	-5.307	0.1091	prot.degrad
	O80860	ATP-dependent zinc metalloprotease FTSH 2, chloroplastic	At2g30950	*M*	-5.312	0.1564	prot.degrad
	Q9SRV5	5-methyltetrahydropteroyltriglutamate--homocysteine methyltransferase 2 (AtMS2)	At3g03780	*S*	-5.356	0.2480	AA met
Slowest	O80934	Uncharacterized protein, chloroplastic	At2g37660	*S*	-6.783	0.2293	N/A
	Q8LE52	Glutathione S-transferase DHAR3, chloroplastic	At5g16710	*S*	-6.816	0.1549	redox
	P25857	Glyceraldehyde-3-phosphate dehydrogenase GAPB, chloroplastic	At1g42970	*M*	-6.861	0.1967	PS.calvin cycle
	Q9XFT3-2	Oxygen-evolving enhancer protein 3-1, chloroplastic (OEE3)	At4g21280	*M*	-6.928	0.2714	PS.light
	Q9SR37	Beta-glucosidase 23	At3g09260	*O*	-7.200	0.2308	CHO hydrolases
	Q9SR37	Beta-glucosidase 23	At3g09260	*M*	-7.218	0.2027	CHO hydrolases
	Q8W4H8	Inactive GDSL esterase/lipase-like protein 23 (Probable myrosinase-associated protein GLL23)	At1g54010	*O*	-7.438	0.1398	2nd met
	Q9SR37	Beta-glucosidase 23	At3g09260	*S*	-7.684	0.6082	CHO hydrolases
	Q9LXC9	Soluble inorganic pyrophosphatase 6, chloroplastic (PPase 6)	At5g09650	*S*	-7.774	1.5988	nucleotide met
	Q9LTQ5	TRAF-like family protein	At3g20370	*O*	-7.976	0.2116	N/A

 doi:10.20944/preprints202405.0780.v1

Q93Z83	TRAF-like family protein	At5g26280	*O*	-8.472	0.5887	N/A
F4IB98	Jacalin-related lectin 11	At1g52100	*O*	-8.879	1.2147	hormone met

[a] Complete list in Supplementary Table S-2. Only proteins with at least 2 unique peptides were used to calculate protein turnover rates. [b]Protein accession number assigned by the UniProt database. [c]The gene identification number assigned by the *Arabidopsis* genome initiative. [d] Three protein fractions: (1) Microsomal enriched protein fraction from the differential centrifugation (1hr, 100,000 × *g* supernatant) of Arabidopsis root or shoot tissue homogenate; (2) Organelle enriched protein fraction from the differential centrifugation (5 min, 1,500 × *g* pellet) of Arabidopsis root or shoot tissue homogenate; (3) Soluble enriched protein fraction from the differential centrifugation (1hr, 100,000 × *g* pellet) of Arabidopsis root or shoot tissue homogenate. [e] Standard deviation of protein turnover rate ($\log_2 k$). [f] Numbers of computable unique peptide. [g] The functional category adapted from MapCave website. [62].

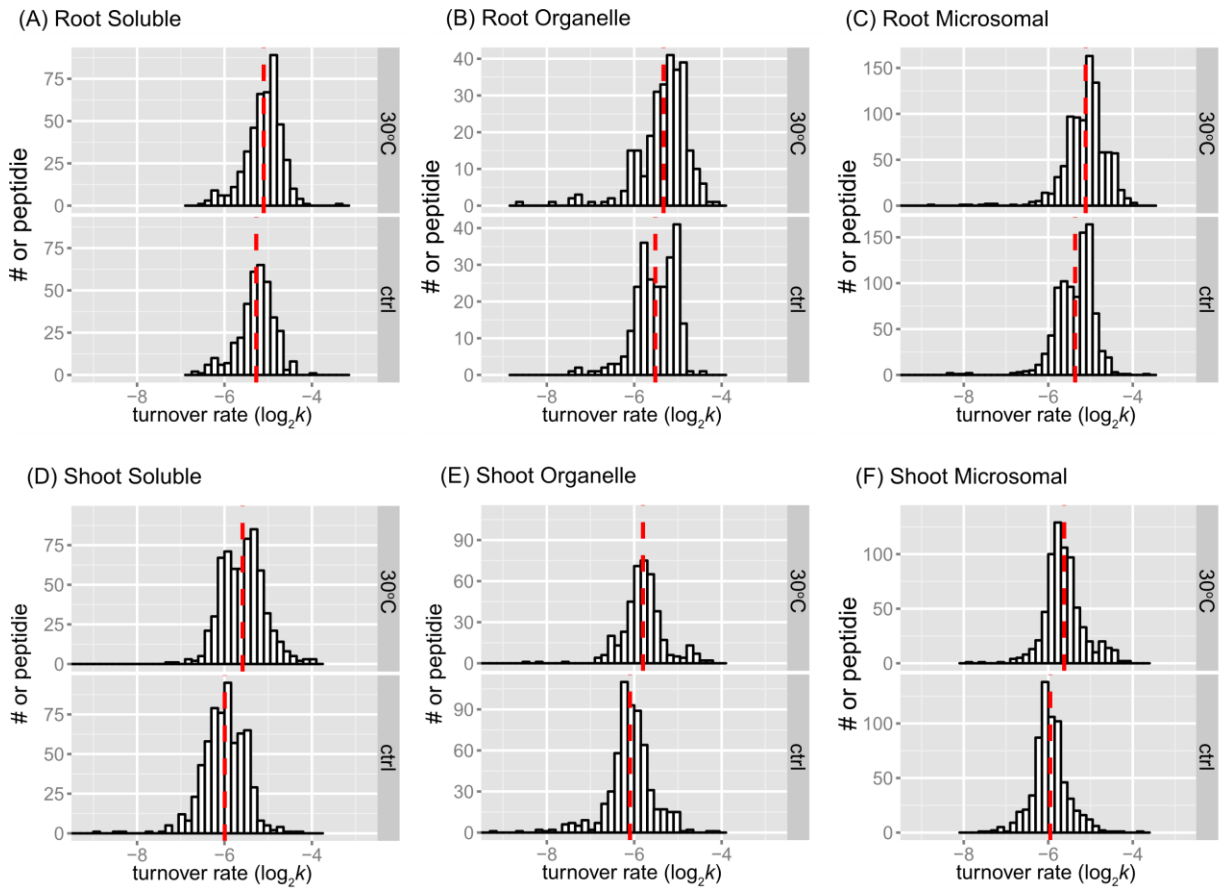

Figure 2. Peptide turnover rate distributions by tissue, fraction, and treatment. Histograms show peptide $\log_2 k$ values plotted for enriched soluble, organelle, and microsomal fractions of root (panels A, B, C) or shoot (panels D, E, and F) tissues. The control (ctrl) and 30°C groups are plotted in the bottom and top frame, respectively. The *y*-axis is the number of peptide counts. The mean value is plotted as the dashed line in red. The bin width is 0.15 for all histograms.

 doi:10.20944/preprints202405.0780.v1

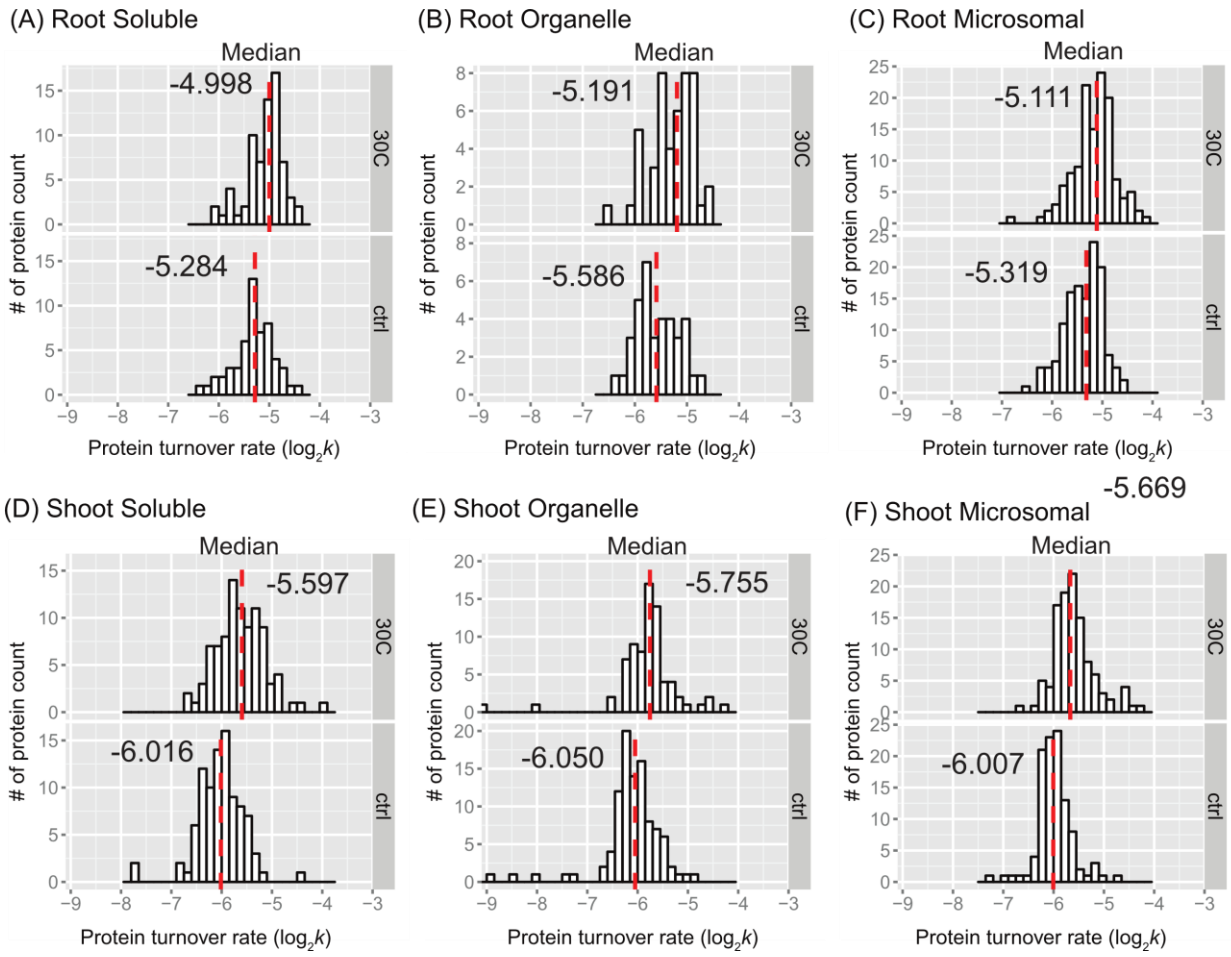

Figure 3. Protein turnover rate distributions by tissue, fraction, and treatment. Histograms show protein log2*k* values plotted for enriched soluble, organelle, and microsomal fraction of root (panels A, B, and C) or shoot (panels D, E, and F) tissues. The control (ctrl) and 30˚C groups are plotted in the bottom and top frame, respectively, The *y*-axis is the number of protein counts. The median value is labeled and plotted as the dashed line in red. The bin width is 0.15 for all histograms.

As the mean may be a more robust population estimator than the median for the bimodal distribution, the mean value was shown in each peptide rate distribution in Figure 2. In every fraction of root or shoot tissue, the average of peptide log2*k* of the 30˚C group was less than that of the control, indicating that peptides tend to turn over faster in response to a higher temperature. The difference in the mean of log2*k* between the control and 30˚C was about 0.17 in the root enriched soluble fraction, 0.18 in the root organelle enriched fraction, 0.25 in the root microsomal enriched fraction, 0.41 in the shoot soluble enriched fraction, 0.30 in the shoot organelle enriched fraction, and 0.33 in the shoot microsomal enriched fraction. Therefore, there was a 1.12~1.18-fold change in the turnover rate of root peptides and a 1.23~1.32-fold change in the turnover rate of shoot peptides at the elevated temperature. At the level of proteins, the fold change of average turnover rate due to 30˚C stress ranged from 1.16 in the root enriched soluble fraction, ~1.31 in the root organelle enriched fraction, 1.22 in the root microsomal enriched fraction, 1.26 in the shoot soluble enriched fraction, 1.23 in the shoot organelle enriched fraction, and 1.34 in the shoot microsomal enriched fraction. Both peptide and protein turnover rate distributions in the three protein fractions indicate that shoot and root proteomes have different scales of response to high temperature. Comparing the change in protein turnover rate between roots and shoots in response to high temperature using ANOVA and Tukey's HSD test revealed a significant difference in log2*k* ($p < 0.001$).

The histograms of some data groups exhibit bell-shaped distributions with slightly asymmetrical patterns in both control and treatment groups. It is possible that the bimodality at the peptide level reflects variations in amino acid content, which could influence peptide turnover rate

 doi:10.20944/preprints202405.0780.v1

calculations. In general, the presence of bimodality is less apparent in the protein turnover histograms (Figure 3) compared to the peptide histograms (Figure 2). This observation is not surprising given the significant decrease in the number of observations from peptides to protein turnover. One potential method to test for bimodality is by employing Hartigan's dip test [35]. In the dip test, the null hypothesis states that the distribution of the sample is unimodal, while the alternative hypothesis suggests that the distribution is not unimodal, indicating at least bimodality. The results from the dip test indicated significant non-unimodal or at least bimodal distribution of peptide turnover rate (k) in the control group of the root microsomal fraction (p-value = 0.00376) and marginally non-unimodal in the root organellar fraction (p-value = 0.0847).

2.2.2. Coefficient of Variation in Protein Turnover as a Function of the Number of Peptide Observations

Figure 4 shows the extent of variation in protein turnover in this experiment as a function of the number of peptide observations that were averaged to produce the rate for each protein. Since the protein turnover rates were obtained as the mean of turnover rates of all selected peptides, the coefficient of variation (CV), also known as relative standard deviation, can be used to show variability in relation to the mean of the population. Here, the values of CV were calculated as the standard deviation divided by the absolute value of protein turnover rate $\log_2 k$. Comparing Figure 4A,B, it appears that both the control and 30˚C datasets have similar levels of variability, suggesting consistency in the protein turnover rates between these two groups. At first, it appears as though the CV values for the protein turnover rates are larger for the rate values calculated from smaller numbers of peptides, but the median CV ranged from 0.02 to 0.05 and is independent of peptide number. The illusion of high CV for small numbers of peptides is due to the inverse correlation between the numbers of rates calculated and the number of peptides used for each calculation. As a result, there are significantly more real outliers for the very well-defined distribution of CV of protein turnover rates from 2 peptides. Most CV values are within the range of 0 to 0.10, while less than ~10 proteins have a CV greater than 0.10. When only 2 peptides were computable for one protein, there were only 3 or 4 cases where the CV was greater than 0.15. Given this analysis of CV, it is quite reasonable to include proteins with turnover rates calculated from as few as 2 computable peptides and to make protein turnover rate comparisons between samples with different numbers of computable peptides.

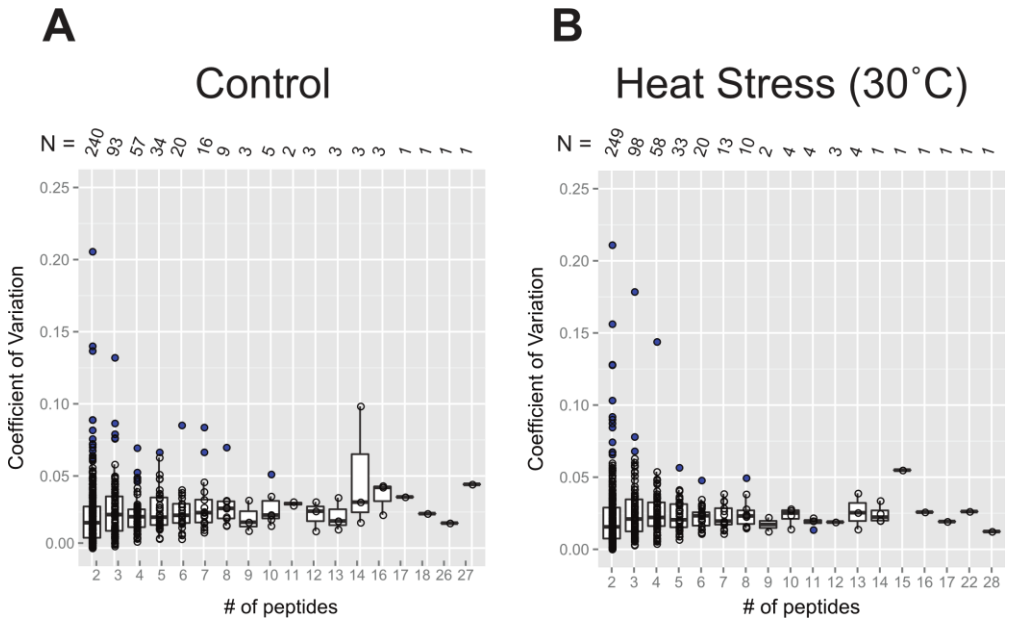

Figure 4. Box plots of the coefficient of variation (CV) of protein turnover rates plotted as a function of the number of peptide rates used in each calculation. The value of CV was calculated from the standard deviation of $\log_2 k$ divided by the mean of $\log_2 k$. The entire dataset used in this plot analysis

 doi:10.20944/preprints202405.0780.v1

includes all unique and shared peptides and is separated based on the treatment group: the control (panel A) and 30˚C (panel B). Boxes show the interquartile range (IQR) of turnover rates of proteins. The error bar represents the entire range of rates and the blue dots represent outliers (1.5 IQR). The number of data points in each x-axis category is given as N, below the x-axis of both plots.

2.2.3. Statistical Significance of Changes in Protein Turnover Rates upon Heat Treatment

Proteomic analysis of protein turnover requires a large number of individual UHPLC-HRMS/MS analyses to provide data across multiple time points, different tissues, different biochemical fractions, and test conditions. These analyses take a considerable amount of time and are expensive. For this reason, it is often impractical to use sampling of biological replicates as a means of testing statistical significance. Furthermore, these analyses often fail to identify many of the lower abundance proteins in replicate runs due to the element of chance in precursor ion detection. As a result, replicated peptide observations are only available for a portion of the identified proteins and typically only those in the top several orders of magnitude in protein abundance. Given the time, cost, and repeatable coverage considerations, a reasonable alternative for determining the significance of changes in turnover rate ($\log_2 k$) between treatments is to apply a linear mixed-effect model (LMM) [36]. An LMM allows one to estimate the likelihood of a difference in $\log_2 k$ values between treatments using a linear model consisting of a mixture of fixed and random effects. The fixed effects represent the errors associated with the conventional linear and non-linear regression portions of the turnover rate derivation, and the random effects represent unknown but random effects such as how peptides were selected from the population of peptides during the UHPLC-HRMS/MS analysis. The LMM approach is also compatible with taking the average of the peptide turnover rate values to determine the protein turnover rate. Supplementary Table S-1 lists the output of the LMM estimation.

Summary of the number of identified peptides and proteins in this study, with the applied threshold for selection, and their number with significant changes in turnover rate ($\log_2 k$) due to the 30˚C treatment ($p < 0.05$) identified in the enriched soluble, organellar, and microsomal fractions of *Arabidopsis* seedling root or shoot tissues are listed in Table S-1. The identified proteins with significant changes in turnover rate ($\log_2 k$) are listed in Supplementary Table S-2, with at least 1 unique peptide in both control and 30˚C samples, which were discussed further (Figures 5, 7 and 8). An overview of the distributions of estimated differences in protein turnover rates between control and heat stress is shown in Figure 5 as histograms (Figure 5A) or box plots (Figure 5B). Overall, proteins enriched in the shoot soluble fraction had the largest change in turnover rate with a median increase of ~0.492 log base 2 scales, or ~1.41-fold increase in protein turnover rate (k) upon heat stress. The box plots in Figure 5B demonstrate that all but the root or shoot soluble fraction had similar variations in the change of protein turnover rate upon heat stress. ANOVA and Tukey's HSD tests revealed that there was a significant difference in the fold change of turnover rate between root and shoot soluble fractions ($p < 0.001$). There were also differences between shoot soluble and shoot organellar fractions ($p < 0.01$) and root soluble and root microsomal fractions ($p < 0.05$). It suggests that the proteins in the shoot tissue exhibit a greater change in rates of turnover in response to high temperature than proteins in the root tissue. Hence, the root proteome may not be as responsive as the shoot proteome to temperature change.

 doi:10.20944/preprints202405.0780.v1

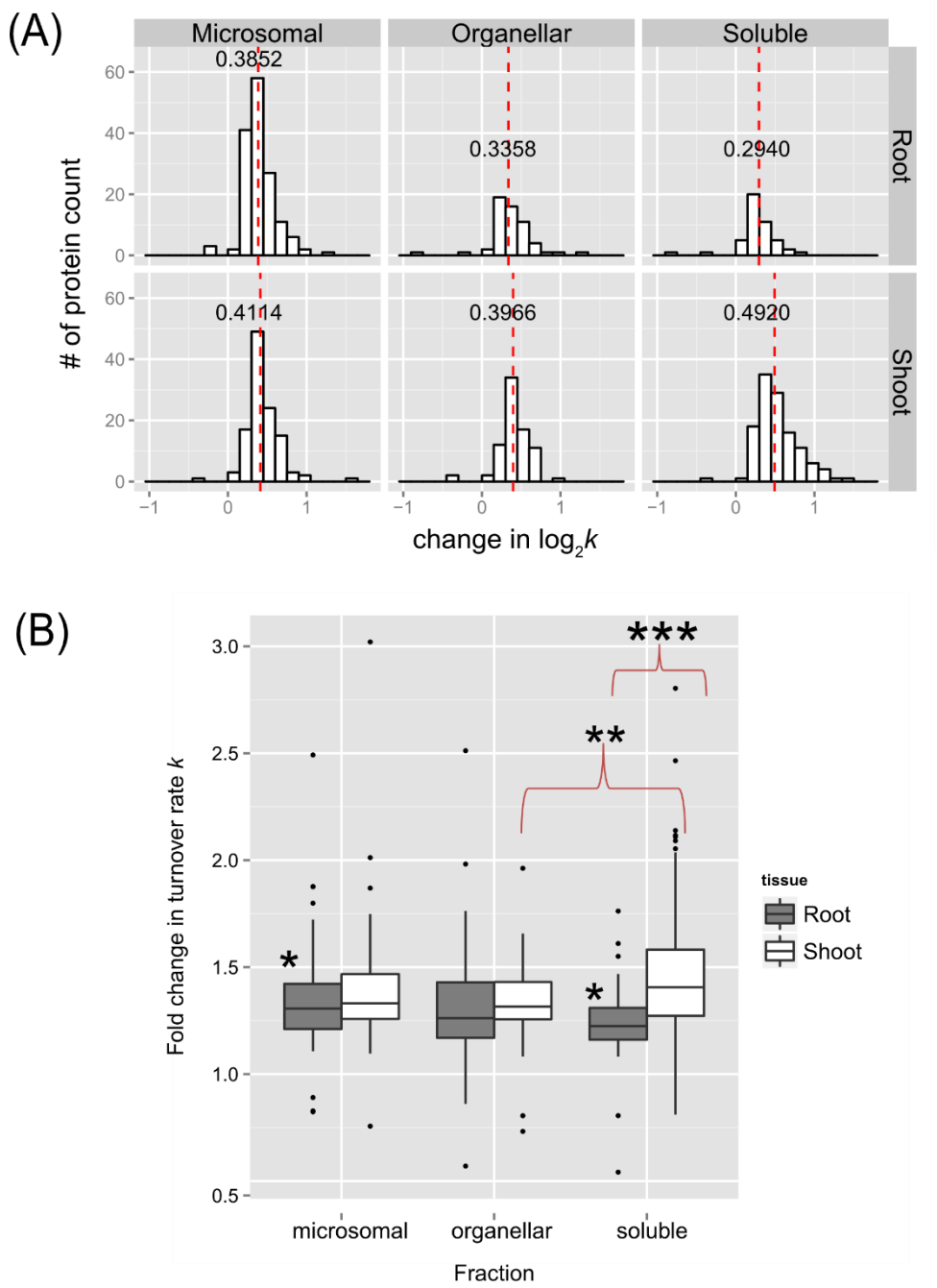

Figure 5. The distribution of changes in protein turnover rates across different tissue and enriched fractions. (A) Histograms showing distributions in the estimated fold change in protein turnover rate (*k*) values in response to 30˚C plotted for soluble, organelle, and microsomal fraction of roots (on the top) or shoots (on the bottom), respectively. The bin width is 0.15 for all histograms. The median value is labeled and plotted as the dashed line in red. (B) Box plots of estimated fold change in protein turnover rate(*k*) in response to 30˚C of protein identified in the root and shoot enriched soluble, organelle, and microsomal fractions. The analyzed data only include proteins with a significant change in $\log_2 k$ ($p < 0.05$) and at least 1 unique peptide in both the control and 30˚C group, which was estimated using an LMM approach after peptide selection criteria were applied. Boxes show the interquartile range (IQR) of change in turnover rates *k*. The error bar represents the entire range of rates and the closed circles represent outliers (1.5 IQR). The estimated changes in turnover rates were analyzed by Tukey's HSD (Honest Significant Difference) test and * for $p < 0.05$, ** for $p < 0.01$, *** for $p < 0.001$.

 doi:10.20944/preprints202405.0780.v1

2.3. Links between Protein Functional Categories and Changes in Protein Turnover Rates upon Heat Treatment

2.3.1. Protein Function and Turnover Rates of Proteins

In a comparison of the shoot and root soluble fractions, the proteins in shoots exhibited a much higher change in turnover rates than in the roots (Figure 5). To determine if function might play a role in protein stability, root and shoot proteins in enriched soluble and membrane fractions from the control experiment were sorted into functional categories. The functional categories were adapted from the MapCave website using the TAIR10 database. Shown in Figure 6 are box and whisker plots of turnover rates of root (panel A) and shoot (panel B) proteins from the control experiment categorized by functional groups. Only proteins with at least 2 unique peptides were reported in Figure 6. For groups with at least 3 proteins, most of them had fairly similar variations in $\log_2 k$ values, such as glutathione S-transferase (GST), protein synthesis, protein targeting, glycolysis, mitochondrial electron chain/ATP synthesis, cellular transport, and stress in root proteins or amino acid metabolism, the light reaction of photosynthesis, the Calvin cycle of photosynthesis, and protein folding in shoot proteins as these categories have well-studied proteins with known function. Some proteins appeared to have more variation in $\log_2 k$ values, especially the ones in the functional categories like redox reaction (ranged from -4.97 to -6.17 in roots, -4.48 to -6.81 in shoots), signaling (-4.89 to -6.12 in roots), development (-4.96 to -6.24 in roots), or secondary metabolism (-4.74 to -7.44 in shoots) as the proteins in these groups are involved in more varieties of function.

Some functional categories exhibited somewhat faster turnover rates, as shown by higher median $\log_2 k$ values in Figure 6. It has been believed that proteins with faster turnover rates could be potential control and regulation points as Heat Shock Proteins (HSPs), proteins involved in signaling, protein synthesis and degradation, and DNA/RNA processing enzymes turned over faster in the proteome turnover study using *Arabidopsis* cell culture; while glycolytic enzymes had the slowest turnover rates. The protein function seems to be related to turnover rates in general in this study. For example, the root proteins involved in cell wall formation, nucleotide metabolism, RNA processes, protein synthesis, hormone metabolism, and stress response had faster turnover rates; while proteins involved in DNA processes, oxidative pentose phosphate pathway, major carbohydrate metabolism, and signaling had slower turnover rates. In the shoot tissue, proteins related to secondary metabolism, protein degradation, and stress response had higher turnover rates and appeared to turnover faster, while proteins involved in the Calvin cycle, hormone, and nucleotide metabolism had much lower turnover rates.

Some specific proteins and their turnover rates were of special interest. Tables 1 and 2 listed the top 10 fastest and slowest proteins in the control experiment of root and shoot tissues, respectively. As listed in Supplemental Table S-2, there was a 4.58-fold difference between the lowest to the highest turnover rate (k) among the identified root proteins (total number 221) while there was a 21.12-fold difference between the lowest to the highest turnover rate among the shoot proteins (total number 297). Therefore, the root proteome appeared to turnover faster but with less variation in general, which suggests there might be a closer correlation in regulating protein synthesis and degradation in root tissue. Stress or redox signaling-related proteins like HSP 70-1 and Chaperone protein dnaJ 3 in roots or HSP 70-11 and Catalase-3 in shoots exhibited relatively rapid turnover. Proteins involved in the light reaction of photosynthesis, especially Photosystem II D2 protein and Photosystem II CP43 reaction center protein, turned over much faster than other proteins functioning in photosynthesis. Therefore, these two proteins might need to be replaced rapidly to maintain normal carbon fixation in plants. Some transport proteins like plasma membrane ATPase 1 (AHA1) and ABC transporter G family member 36 (ABCG36; PEN3; PDR8) in the root tissue were identified as outliers in the box plot due to their extraordinarily fast turnover rates. It has been shown that the expression of *ABCG36*/*PEN3*/*PDR8* gene in seedlings is 5 to 40-fold higher than other ABC transporters and its transcript abundance in leaves is comparable with transcript levels of some housekeeping genes like cytosolic glyceraldehyde-3-phosphate, suggesting the multiple physiological functions of ABCG36/PEN3/PDR8. It has later been reported that ABCG36/PEN3/PDR8 is an ATP-binding

 doi:10.20944/preprints202405.0780.v1

cassette (ABC) transporter localized on the plasma membrane and is thought to efflux indole-3-butyric acid (IBA) in root tips, several biotic, and abiotic stress responses. The fast turnover rate of ABCG36/PEN3/PDR8 in seedling roots could result from the high level of protein synthesis, supporting its multiple roles in heavy metal ion tolerance as well as regulating the IBA-mediated homeostasis of auxin in roots. On the other hand, some glycosyl hydrolase family proteins, such as beta-glucosidase 22 (BGLU22) or beta-glucosidase 23 (BGLU23/PYK10) in the root or shoot tissue had the slowest turnover rates. BGLU family proteins are important for ER formation and their hydrolytic activity for glucoside that accumulates in the roots of *Arabidopsis* has been believed to be important in defense against pests and fungi. It has been proposed that healthy seedling roots accumulate beta-glucosidases in the ER bodies. Therefore, when plant cells are under attack from herbivores or pathogens, beta-glucosidases leak from the ER body and bind to GDSL lipase-like proteins (GLLs) and Jacalin-related lectins in the cytosol to form complexes with increased enzyme activity which hydrolyzes glucosides to produce toxic compounds like scopolin. These proteins are very abundant and expressed exclusively in *Arabidopsis* seedlings, so their slowest turnover rates identified in this study suggest that BGLU22 and BGLU23 act like housekeeping proteins in *Arabidopsis* seedlings in order to rapidly trigger defense mechanism on demand.

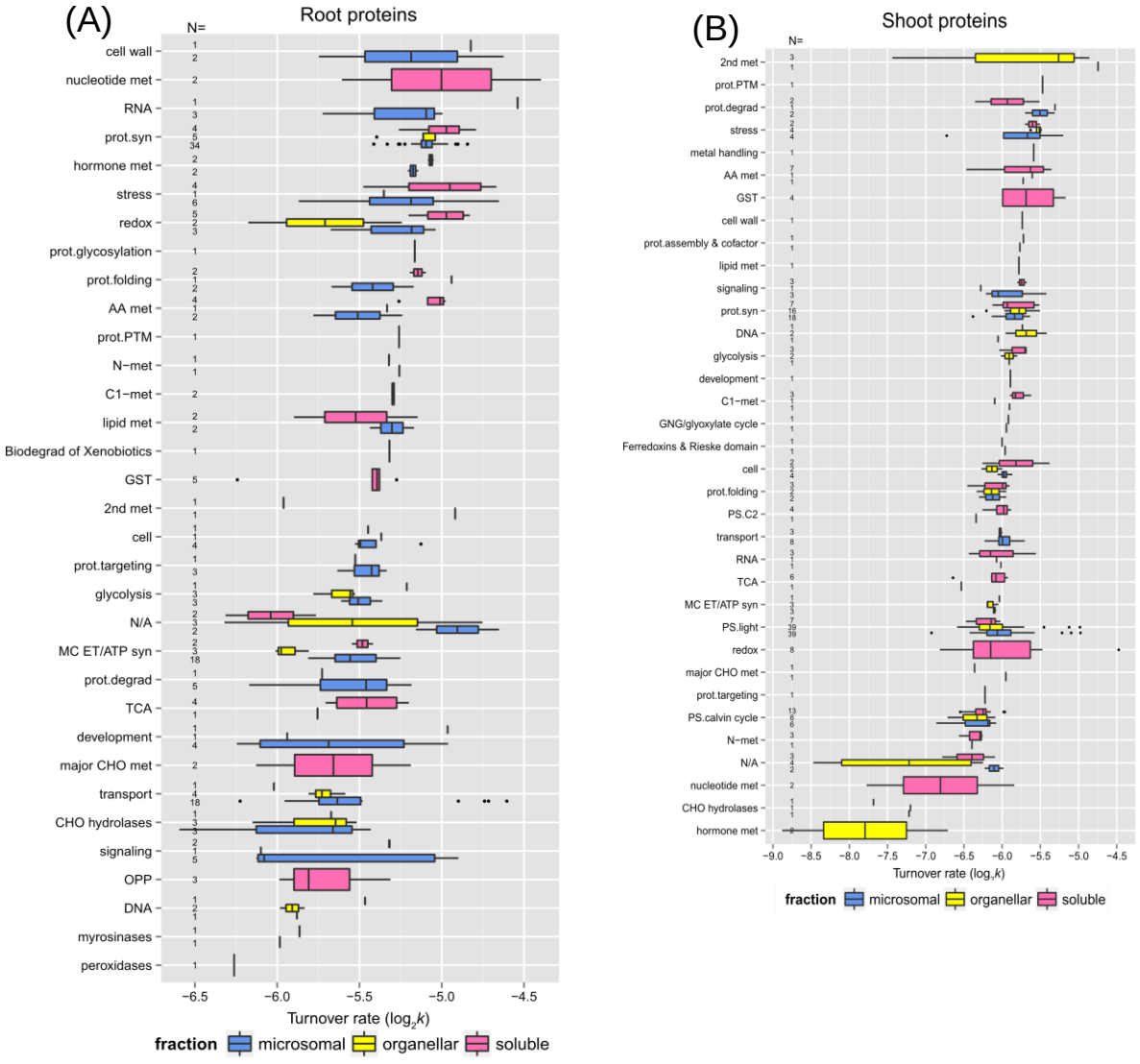

Figure 6. The relationship between protein function and protein turnover rates. Box plots of protein turnover rate $\log_2 k$ for root (Panel A) and shoot (Panel B) proteins from the control experiment are sorted by functional categorization, which was adapted from the MapCave website (http://mapman.gabipd.org/web/guest/mapcave) using TAIR10 database, with outliers shown as closed circles. The used data only include proteins at least 2 unique peptides. The number of proteins

 doi:10.20944/preprints202405.0780.v1

in each function category is given as *N*, along the y-axis of both plots. The protein count of each function group is also labeled in the plot. Abbreviations: 2nd met, secondary metabolism; AA met, amino acid metabolism, C1-met, single carbon metabolism; DNA, CHO hydrolases, miscellaneous gluco-, galacto- and mannosidases; DNA processing; Glc-, Gal- & mannosidases, glucosyl-, galactosyl- & mannosyl- glycohydrolases; GNG, gluconeogenesis; GST, glutathione S-transferases; lipid met, lipid metabolism; major CHO met, major carbohydrate metabolism; MIP, major-intrinsic proteins; MC. ET/ATP syn, mitochondrial electron transport/ATP synthesis; N-met, nitrogen metabolism; OPP, oxidative pentose phosphate pathway; prot.assembly, protein assembly & cofactor ligation; prot.degrad, protein degradation; prot.folding; protein folding; prot.targeting, protein targeting; prot.PTM, protein post-translational modification; prot.syn, protein synthesis; PS.C2, photorespiration; PS.light, the light reaction of photosynthesis; PS.calvin cycle; the Calvin Cyle of photosynthesis; RNA, RNA processing; S-assimilation, sulfur assimilation; TCA, tricarboxylic acid cycle.

2.3.2. Protein Function and Change in Turnover Rates due to High Temperature

To further explore functional correlations with protein turnover changes during heat stress, the proteins with significant changes due to high temperature identified in this study were also sorted into functional categories. Figure 7A and B are box plots showing the fold changes in turnover rate in response to the higher temperature treatment (calculated from the estimated difference in $\log_2 k$ between the control and 30˚C using the LMM fit) across functional categories for each tissue and fraction. Only proteins with a significant change in $\log_2 k$ ($p < 0.05$) and at least 1 unique peptide in both control and 30˚C groups were included in this analysis. In each plot, the protein categories were sorted on the y-axis from largest to smallest median difference in protein $\log_2 k$. Functional categories with only 1 data point (1 protein) were included in the plot to provide additional coverage of the functional categories. The number of proteins in each functional category is given as N along the y-axis of each plot. Most of the groups had median values ranging from 1.25 to 1.75 fold change. Among those identified in roots, proteins involved in redox signaling pathways, stress response, protein folding, and calcium-signaling pathways had the largest median changes in turnover rate. In shoots, the beta-glucosidase family and proteins sorted in photorespiration, protein folding, stress response, hormone, and secondary metabolism exhibited the largest median changes in turnover rate due to heat (~1.5 fold change in k).

In the functional categories identified in both root and shoot soluble fractions such as redox signaling, stress response, protein degradation, and glutathione S-transferase metabolism, shoot proteins exhibited greater changes in turnover rates than root proteins, as well as secondary metabolism, protein synthesis, and stress response in the enriched organellar and microsomal fractions (Figure 7B,C). On the other hand, proteins assigned to the glycolysis, cellular transport, mitochondrial electron chain/ATP synthesis functional group, TCA cycle, signaling, cell organization, and cell wall structure displayed similar changes in turnover rate with heat stress in both roots and shoots, suggesting that the turnover of proteins involved in these biological processes such as mitochondrial ATP synthesis is regulated uniformly throughout the whole seedling.

Comparing the changes in turnover rates of proteins within the same functional category between different root (Figure 8A) or shoot (Figure 8B) fractions could help identify specific proteins with different levels of responses to heat stress due to compartmentalization. For example, shoot proteins involved in photorespiration appeared to be more affected by high temperature in the soluble fraction than in the membrane fractions in general. However, after inspection of the proteins listed in Supplementary Table S-2, exceptions such as Glycolate oxidase 1 (GOX 1; At3g14420), which was identified in both soluble and microsomal fractions, turned over fairly rapidly in both fractions. Other categories such as the light reaction of photosynthesis, cellular transport, cellular organization, mitochondrial electron transfer/ATP synthesis, protein synthesis, and glycolysis exhibited a similar breadth of responses across different fractions. This may be due to the fact that these proteins were relatively abundant so they are being isolated in multiple fractions. Choroplastic ATP synthase subunit alpha (Atcg00120), for example, was identified in all three fractions.

 doi:10.20944/preprints202405.0780.v1

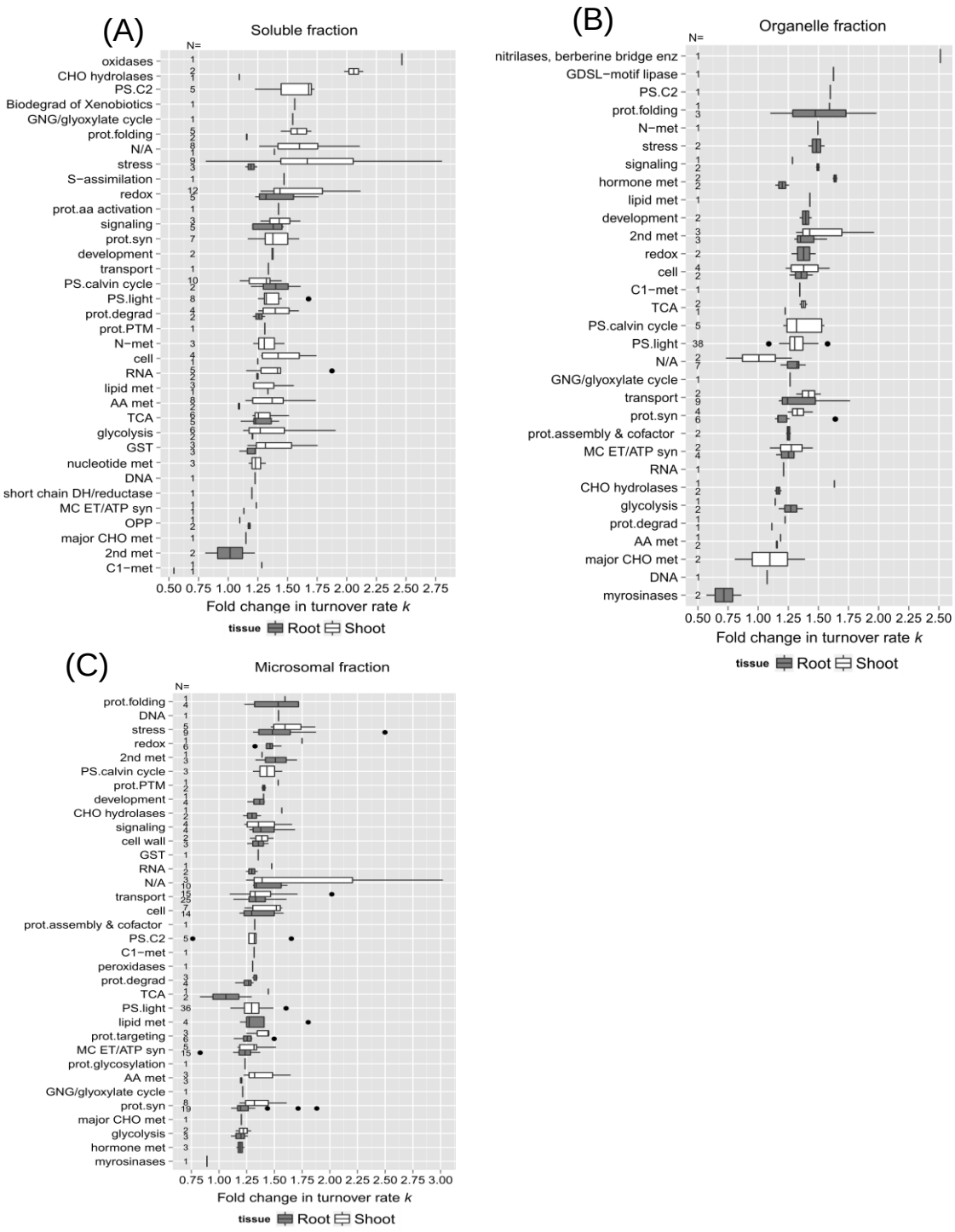

Figure 7. The relationship between protein function and change in turnover due to elevated temperature. Box plots of the estimated change in $\log_2 k$ in response to 30˚C (diffs. in $\log_2 k$) for root and shoot proteins are sorted by functional categorization, which was adapted from the MapCave website using TAIR10 database, with outliers shown as closed circles. (A) Soluble enriched fraction of root or shoot tissue homogenate. (B) Organelle enriched fraction of root or shoot tissue homogenate. (C) Microsomal enriched protein fraction of root or shoot tissue homogenate. The used data only include proteins with a significant change in $\log_2 k$ ($p < 0.05$) and at least 1 unique peptide in both the control and 30˚C groups. The number of proteins in each function category is given as *N*, along the y-axis of all plots.

Preprints.org (www.preprints.org) | NOT PEER-REVIEWED | Posted: 13 May 2024 doi:10.20944/preprints202405.0780.v1

Figure 8. Comparison of protein functions with the change of turnover rates in response to 30˚C between different protein fractions. Boxes show the interquartile range (IQR) of the estimated difference in $\log_2 k$ turnover rates of proteins (diffs in $\log_2 k$). Proteins are sorted in functional categorization, comparing results between the enriched soluble, organelle, and microsomal fraction of root (panel A) or shoot (panel B) tissues. The error bar represents the entire range of rates and the closed circles represent outliers (1.5 IQR).

3. Discussion

 doi:10.20944/preprints202405.0780.v1

In this study, an elevated temperature of 30˚C was applied for durations ranging from 8 to 48 hours. Despite being relatively moderate compared to typical heat stress studies, it has been demonstrated that even a modest change in temperature, such as transferring 12-day-old *Arabidopsis* seedlings from 12 to 27˚C for 2 hours, can significantly alter the expression of over 5000 genes by at least 2-fold [37]. The present study's moderate heat treatment aligns with the moderately elevated temperature, contrasting with the heat stress conditions in the Mittler study [37]. This suggests that different heat sensors and signaling pathways may perceive these temperature regimes differently.

Results of this study suggest that heat stress causes a greater change in shoot proteome than root proteome. In plants, it is believed that root growth is more sensitive to acute heat stress than shoot growth as the high soil temperature is more detrimental than the high air temperature and lower soil temperature could help plants survive when grown under high air temperature [38]. Significant changes in the turnover rates of HSP70, HSP90, and the chaperone protein htpG underscore their protective roles against heat-induced protein degradation. Specifically, HSP90-5 is crucial for maintaining chloroplast integrity under stress. RuBisCO activase exhibited increased turnover, suggesting limitations in photosynthetic efficiency at higher temperatures. Proteins like GSTs, catalases, and peroxidases involved in redox homeostasis showed diverse responses, indicating their roles in oxidative stress management. Notable changes in proteins such as GDSL esterase/lipase and 14-3-3 family proteins highlight their involvement in broader stress responses and signaling pathways related to abscisic acid and brassinosteroids.

Future research should focus on understanding the mechanisms behind the differential proteomic responses to moderate heat stress, particularly comparing resilience mechanisms in roots versus shoots. Employing advanced techniques like metabolic flux analysis [39–41] would be key for quantifying metabolic changes and linking them to specific biochemical pathways, enhancing our understanding of plant metabolic adjustments to heat stress. Additionally, integrating systems biology approaches to correlate transcriptomic, proteomic, and metabolomic data could provide comprehensive insights into the regulatory networks and pathways activated during heat stress, potentially revealing critical regulatory nodes for enhancing plant heat tolerance [42–44].

3.1. Heat Shock Proteins (HSPs) and Chaperones

It has long been known that the expression of stress proteins like HSPs could be induced by heat shock at almost all stages of development, and the induction of HSPs seems to be a universal response to heat stress among organisms [45]. In the results, HSPs appear in the stress protein functional category (Table 5). While it is clear that most of the proteins listed in the table are specifically related to heat stress, such as HSP70-1, HSP70-3, HSP70-11, HSP90-2, HSP90-3, and the chaperone protein htpG family, in several of the fractions, there are additional potential stress response-related proteins predicted from the microarray gene expression data, such as RD2 protein (involved in the response to desiccation), major latex protein (MLP)-like proteins 328 and 34 (responsive to biotic stimulus), MLP-like protein 34, Dehydrin COR47 (responsive to cold), and At4g23670 protein (involved in the response to salt stress and bacterial infections). Interestingly, the root soluble fraction HSPs and stress-related proteins had smaller increases in turnover rate compared with other fractions. This significantly smaller increase in HSP and stress-related protein turnover for the root soluble protein fraction may help explain the generally much smaller change in turnover rate in that fraction compared with the other fractions.

A previous study found that stress response proteins such as heat shock chaperones and proteins associated with oxidative stress have relatively high degradation rates, although that study was performed using an enriched mitochondrial fraction of *Arabidopsis* suspension cells [28]. While it is risky to extrapolate from this prior study to intact plants, it is reasonable to postulate that the rapid turnover rate could be even more dramatic in planta. As HSPs help to prevent protein degradation, the aggregation of HSPs into a granular structure in the cytoplasm helps to protect the protein biosynthesis machinery from denaturation [6]. Our study indicates the shoot HSP90-5 (Chaperone Protein htpG family Protein; At2g04030) had a 2.05-fold increase in k in response to heat. Overexpression of HSP90-5 in *Arabidopsis* has been shown to result in reduced plant tolerance to

 doi:10.20944/preprints202405.0780.v1

drought, salt, and oxidative stress, while knocking out the HSP90-5 gene results in an embryo lethal phenotype, indicating that HSP90-5 is an essential gene [46]. It has been shown that HSP90-5 is important in maintaining the integrity of chloroplast thylakoid formation [46]. These findings, along with the dramatic change in the turnover rate of HSP90-5 when treated with high temperature in this study all suggest that properly controlled expression of HSP90-5 is important for plant growth and chloroplast biogenesis. HSPs like HSP70, HSP90, and HSP60 belong to molecular chaperone families. Molecular chaperones bind and catalytically unfold misfolded and aggregated proteins as a primary cellular defensive and housekeeping function [47]. Other proteins with significant changes in turnover rate in response to high temperature are also involved in protein degradation and protein folding functions, including several proteinases and multiple chaperones (Supplementary Table S-1 & Figure 7), including mitochondrial and chloroplast Chaperonin *CPN60* (HSP60) and CPN-10, which turnover rapidly in response to heat. Plastidic *CPN60* alpha and beta are required for plastid division in *Arabidopsis* and *CPN60* are required to be maintained at a proper level for folding of stromal plastid division proteins and are essential for development in chloroplasts [48]. The observed change in *CPN60* turnover rates is somewhat correlated to the study revealing the slightly reduced expression of CPN-60 in seedling shoots when encountering the elevated temperature at 28˚C [48]. Another chaperone protein AtBAG7 (At5g62390) exhibited a faster turnover rate at elevated temperature. AtBAG7 is required to maintain the c and is localized in the endoplasmic reticulum, which is unique among BAG family members[15]. It has been proposed that activity may be regulated post-translationally, given that its gene expression does not appear to be affected by heat or cold stresses [15]. Since AtBAG7 directly interacts with an HSP70 paralog, AtBAG7 activity is likely regulated post-translationally through modulation of protein turnover [15].

3.2. Photosynthesis and Carbon Assimilation

As temperature is a crucial factor affecting photosynthetic activity in plants, as expected, proteins involved in photosynthesis, including components of photosystems I & II (PSI & PSII), the cytochrome b6-f complex, chloroplast ATP synthase, and the Calvin cycle, were identified for having varying degrees of change in turnover in response to heat. Prior heat stress-related studies found that the oxygen-evolution complex (OEC) of PSII is the main target of heat stress [49]. From this study, changes in turnover rates of OEC subunits were around 1.21-1.42 fold, similar to the majority of the proteins involved in photosynthesis, in response to heat (Supplementary Table S-1). There were extreme cases like RuBisCO activase (At2g39730) and chlorophyll a/b binding protein (LHCB6; At1g15820) that exhibited larger, 1.57 and 1.60 fold changes in k, respectively. As it is highly sensitive to heat denaturation, RubisCo activase is thought to be a key element involved in mediating the heat-dependent regulation of carbon assimilation as it could limit the photosynthetic potential of plant tissues at high temperatures [12]. Although the enzyme activity of RubisCo activase was not decreased until the temperature was higher than 37˚C in cotton and tomato leaves [12], our study suggests that this enzyme in *Arabidopsis* seedlings could "sense" relatively mild elevated temperatures like 30˚C in terms of protein turnover. It is hard to judge from the results whether the turnover rates of proteins of PSII and light-harvesting complex II (LHCII) were more affected by high temperature than PSI, as it has long been believed that PSII is more vulnerable to elevated temperature [50,51]. A comparison, however, of the differences between PSI and PSII protein turnover following heat stress should indicate the relative heat tolerance of the two photosystems under mild elevated temperature conditions. To this end, LHCB6, which is associated with PSII, turns over significantly faster (1.60 fold change in k) after heat treatment than the Photosystem I reaction center subunit III (1.25 fold change in k). Notably, these rate changes are on the high and low extremes of the range of changes observed for protein components of photosynthesis. LHCB6 is a monomeric antenna protein of PSII, participating in zeaxanthin-dependent photoprotective mechanisms, and is therefore thought to be specialized in enhancing photoprotection under excess light conditions. The presence of the protein is often associated with the adaptation of plants to terrestrial ecosystems [52]. Heat stress at temperatures around 38-40˚C has been demonstrated to cause structural changes in the thylakoid membranes, as well as increased phosphorylation of LHCIIs and PSII core subunits, migration of

 doi:10.20944/preprints202405.0780.v1

phosphorylated LHCII from the grana stacks to the stroma lamellae, and cyclic electron flow within PSI [53]. It will be interesting to study if the change in LHCB6 turnover could be related to the above observations at 40˚C even when mild temperature conditions like 30˚C are employed.

3.3. Redox Homeostasis: HSPs, Catalases and Peroxidases

The turnover rates of proteins involved in the production of reactive oxygen species (ROS) were also affected by high temperatures. These include several different types of HSPs, catalases, and peroxidases. An additional group of antioxidant enzymes, including GST, DHAR, and thioredoxins, exhibited significant heat-related changes in turnover (Supplementary Table S-1). Among those, GST class Tau-member 19 (GSTU19; At1g78380), the most abundant GST in *Arabidopsis*, exhibited the smallest difference in turnover rate (1.31-fold change) in roots but showed a much larger difference (1.75 fold change) in turnover rate in shoots.

Hydrogen peroxide (H_2O_2) is an important signaling molecule in plant environmental responses, and heat shock-induced H_2O_2 accumulation is required for efficiently inducing the expression of small HSP and ascorbate peroxidase genes (*APX*1 & *APX*2) [54]. Among several types of H_2O_2-metabolizing proteins, catalases are highly active enzymes that do not require cellular reductants as they catalyze the dismutation reaction of two molecules of H_2O_2 to generate one molecule of O_2 and two of H_2O. A 1.40-fold change in turnover rate *k* was observed for catalase-3 (CAT3; At1g20620) in shoots upon temperature elevation. APXs are also known to be important H_2O_2-scavenging enzymes, but they use ascorbate as an electron donor. Their function is tightly linked to ROS signaling pathways and the regulation of cellular ROS levels [54]. In this study, there was a moderate increase in APX1 (At1g07890) turnover rates under heat stress conditions in both root and shoot tissues. *APX1* is expressed in roots, leaves, stems, and many other tissues [55], and mutation in *Arabidopsis APX*1 exhibits increased accumulation of cellular H_2O_2 and suppressed growth and development [56]. It has been reported that *APX*1 activity could be partially inhibited in roots through modification by S-denitrosylation in an auxin-dependent manner [57]. APX1 could be an interesting research target to explore the links between nitric oxide (NO), H_2O_2, auxin hormone signaling, and heat stress.

3.4. Special Cases: Decreases (Negative diff.log$_2$k) or Major Increases in log$_2$k in Response to Heat

3.4.1. GDSL Esterase/Lipase Family

GDSL esterase/lipase 22 (GLL22; At1g54000) showed slightly reduced turnover rates in both root organellar and microsomal fractions (fold change in *k* about 0.86 and 0.89, respectively), indicating that GLL22 becomes more stable and/or with reduced transcription or translation when transferred to 30˚C. It has been proposed that under pathogen or herbivore attack, GLL22 may aggregate with beta-glucosidases (BGLU 21, 22, and 23), and other Jacalin-related lectins (JALs) in the cytosol [58]. It is possible that under temperature stress, GLL22 turns over slower due to being recruited into more stable complexes. The change in turnover rates of the BGLU protein family, on the other hand, had a wide variation across root or shoot protein fractions (1.09 ~ 2.14 fold change due to heat). BGLU proteins appeared to turn over faster in shoots than in roots, thus the turnover rates of BGLUs in shoots could be more affected by heat stress than BGLUs in roots. Similar results were observed for JAL proteins like Jacalin-related lectin 30 (PYK10-binding protein 1; At3g16420), Jacalin-related lectin 33 (JAL 33; At3g16450), and Jacalin-related lectin 34 (JAL 34; At3g16460), whose turnover rates also had a greater change in shoots than roots when under heat stress, suggesting these stress-responsive proteins in shoots may be compromised when plants encounter heat stress.

3.4.1. 14-3-3 & v-, p-type ATPase

It is intriguing to observe signaling proteins like 14-3-3 family proteins and proton pump v- and p-type H+-ATPases with significant changes in turnover rate due to elevated temperature because of their known roles in ABA signaling in response to abiotic stress. Increased H_2O_2 production under multiple different abiotic stress conditions has been shown to result in elevated levels of ABA, which may in turn be involved in the induction of the temperature stress response in plants [14]. Plant 14-

 doi:10.20944/preprints202405.0780.v1

3-3 family proteins function in a wide range of cellular processes. Two 14-3-3 proteins show fairly large changes in protein turnover in response to heat stress: 14-3-3-like Protein GF14 mu (General regulatory factor 9; At2g42590), and 14-3-3-like Protein GF14 epsilon (General regulatory factor 10; At1g22300) with 1.61 and 1.45 fold changes respectively. It has been discovered that 14-3-3 mu participates in light sensing during early development through phytochrome B signaling and affects the time of transition to flowering via interaction with CONSTANS [59]. As T-DNA mutants of the 14-3-3 mu gene exhibit shorter root lengths and a dramatic increase in the numbers of chloroplasts in the roots [60], it is possible that its difference in heat stress response between root and shoot tissues is related to its role in chloroplast development. On the other hand, the 14-3-3 epsilon protein may be involved in brassinosteroid (BR) signaling, like 14-3-3 lambda protein, as the 14-3-3 epsilon protein has been shown to interact with the BZR1 transcription factor in a yeast-two hybrid screen [61]. Therefore, these proteins involved in signal transduction may be affected by heat stress thus influencing the BR hormone regulation.

4. Materials and Methods

Materials

Distilled, deionized water was prepared with a Barnstead B-pure water system (Thermo Scientific, Waltham, MA). Acetonitrile (CHROMASOLV® Plus for HPLC, ≧99.9%), formic acid (ACS reagent ≧96%), and acetone (CHROMASOLV® Plus for HPLC, ≧99.9%) were obtained from Sigma-Aldrich (St. Louis, MO). Triton X-100 was obtained from ICN Biochemicals Inc. (Ohio, USA). 99 atom% $K^{15}NO_3$ and 98 atom% $Ca(^{15}NO_3)_2$ were obtained from Cambridge Isotopes Laboratories, Inc. (Andover, MA). Sequencing grade modified trypsin was purchased from Promega (Madison, WI). Pierce C18 Spin columns were obtained from Thermo Scientific (Pierce Biotechnology, Thermo Scientific, Rockford, IL). Micro-centrifuge tubes used for the proteomics study in this thesis were "Protein LoBind Tube 1.5 mL", obtained from Eppendorf AG (Hamburg, Germany). Nylon filter membranes (mesh opening 20 μm, Cat. #146510) were obtained from Spectrum Laboratories Inc. (Rancho Dominguez, CA).

Plant Growth and Labeling Conditions

Arabidopsis thaliana ecotype Columbia Col-0 was used for all experiments. Seeds were sterilized with 30% (v/v) bleach containing 0.1% (v/v) Triton X-100 and vernalized at 4˚C for two days, *Arabidopsis* seeds were germinated on a nylon filter membrane placed on the top of ATS agar plates. The seedlings were grown under continuous fluorescent light (~80 μmole photon m^{-2} s^{-1}) at 22˚C for 8 days. For the heat-treated group, these 8-day-old seedlings along with the nylon membrane (mesh opening 20 μm, Cat. #146510, Spectrum Laboratories Inc., Rancho Dominguez, CA) were then transferred onto fresh ATS [63] media containing 99 atom% $K^{15}NO_3$ and 98 atom% $Ca(^{15}NO_3)_2$ (Cambridge Isotopes Laboratories, Inc., Andover, MA) (^{15}N-medium) and then transfer to the 30˚C growth chamber. For the control group, seedlings were continuously grown at 22˚C after being transferred to the ATS medium with the normal nitrogen source (^{14}N-medium).

For both the control and high-temperature groups, crude proteins were extracted at 0, 8, 24, 32, and 48 hours after ^{15}N incorporation (time 0 samples were shared by both groups). Prior to transferring seedlings from ^{14}N- to ^{15}N-media, the ATS liquid medium lacking $K^{15}NO_3$ or $Ca(^{15}NO_3)_2$ was used to rinse the seedlings.

Proteomic Sample Preparation

For the proteomic analysis of *Arabidopsis* seedlings, hypocotyl and cotyledons (as "shoot" samples) were dissected from root tissues. From root and shoot tissues, soluble and membrane proteins were extracted and enriched by differential centrifugation as described previously by Fan *et al.*[33] in the stable isotope incorporation experiments. Soluble proteins (150 μg) were precipitated by the addition of ice-cold acetone to 80% (v/v) followed by overnight incubation at –20˚C. The protein precipitate was then pelleted by centrifugation for 15 min at 16,000 g. The air-dried pellets were

 doi:10.20944/preprints202405.0780.v1

dissolved in 8 M urea/8 mM DTT and added to a final protein concentration of 8 μg/μL. The proteolysis of soluble protein, membranous protein fractions derived from 1,500 × g (organelle), and 100,000 × g (microsomal) pellets were processed as described previously [33]. The resulting peptides obtained from soluble or membrane protein fractions were purified by C18 solid phase extraction using the C18 Spin column (Pierce Biotechnology, Thermo Scientific, Rockford, IL) and per the manufacturer's protocol. After purification, peptides were concentrated under vacuum to dryness using a SpeedVac concentrator (Savant) and were re-suspended in 5% (v/v) acetonitrile, 0.1% formic acid prior to ultra-high performance liquid chromatography–high-resolution tandem mass spectrometry (UHPLC-HRMS/MS) analysis.

UHPLC-HRMS/MS Analysis

The tryptic peptides were analyzed by UHPLC-HRMS/MS using a Q Exactive hybrid quadrupole orbitrap mass spectrometer with an Ultimate 3000 UHPLC inlet (Thermo Fisher Scientific, CA) equipped with an ACQUITY UPLC BEH C18 reversed-phase column (Waters, 2.1 mm x 100 mm, 1.7 μm particle size). Solvent A (0.1% (v/v) formic acid in H_2O) and B (0.1% (v/v) formic acid in acetonitrile) were used as mobile phases for gradient separation. The equivalent of 30 μg of soluble protein digest, 10 μg of organellar protein digest, or 30 μg of microsomal protein digest were loaded separately onto the column in 5% solvent B for 12 min at a flow rate of 0.3 mL/min, followed by elution by gradient: 2 min from 5% B to 10% B, 60 min to 40% B, 1 min to 85% B and maintained for 10 min. The column was equilibrated for 15 min with 5% B prior to the next run. The MS/MS data were collected in a data-dependent acquisition mode similar to Sun et al. [64] with minor modifications. Full MS scans (range 350−1800 m/z) were acquired with 70K resolution. The target value based on predictive automatic gain control (AGC) was 1.0E+06 with 20 ms of maximum injection time. The 12 most intense precursor ions ($z \geq 2$) were sequentially fragmented in the HCD collision cell with a normalized collision energy of 30%. MS/MS scans were acquired with 35k resolution and the target value was 2.0E+05 with 120 ms of maximum injection time. The ion selection threshold of 1.0E+04 and a 2.0 m/z isolation width in MS/MS were used. The dynamic exclusion time for precursor ion m/z was set to 15 sec.

Protein Identification

All .raw files were converted to mzXML files by the msConvert3 tool of ProteoWizard[65] and then converted to mgf format by MGF formatter (v0.1.0). OMSSA (v2.1.9)[66] was used for database searching against the UniProt Arabidopsis thaliana database (accessed on February 2013, 33,311 sequences, http://www.uniprot.org) combined with the contamination list from the cRAP database (common Repository of Adventitious Proteins, accessed on February 2013, 115 sequences, http://www.thegpm.org/crap/) and reversed sequences. The search parameters were: 6 ppm precursor ion mass tolerance, 0.02 m/z product ion mass tolerance, methionine oxidation as variable modification, and a maximum missed cleavage of 2. The search results were then analyzed by Scaffold (v3.6.5, Proteome Software Inc., Portland, OR)[67] to validate MS/MS-based peptide and protein identifications. The results were filtered with a false discovery rate of less than 0.5% on the peptide level and 1% on the protein level with a minimum of two unique peptides required for identification. Proteins that contained similar peptides and that could not be differentiated based on MS/MS analysis alone were grouped to satisfy the principles of parsimony. All the above activities of data conversion and protein database searching were performed on the Galaxy-P platform (https://galaxyp.msi.umn.edu/) [68–70], and supported by the Supercomputing Institute at the University of Minnesota). The mass spectrometry proteomics data have been deposited to the ProteomeXchange Consortium (http://proteomecentral.proteomexchange.org) via the MassIVE partner repository (the dataset identifiers will become available once the manuscript is accepted).

Calculation of Protein Turnover Rates

 doi:10.20944/preprints202405.0780.v1

The workflow of using the *ProteinTurnover* algorithm is described in the following steps: (1) Data preparation. The Scaffold spectrum report (CSV format) and all MS data (mzXML format) were uploaded for access by the R script; (2) Parameter settings. Parameters such as stable isotope (^{15}N) used for labeling, experimental design (incorporation), peptide ID confidence threshold (80), spectral fitting model (beta-binomial), and nonlinear regression setting ($\log_2 k$) were defined; (3) Outputs generated. After finishing the analysis of a dataset, the results were compiled in a summary HTML file, which includes model plots (spectral fitting by MLE), EIC plots, and regression plots (relative abundance fits) for each individual peptide to be used as needed for manual inspection. The *ProteinTurnover* R script also generates a spreadsheet (.csv) containing peptide turnover information, which includes the peptide amino acid sequences, protein UniProt accession numbers (ID), visual scores, $\log_2 k$ values, and standard errors of $\log_2 k$.

For isotope label incorporation experiments, the $\log_2$ value for each turnover rate constant ($\log_2 k$) of each peptide was calculated by performing a non-linear regression of the distribution abundance ratios of unlabeled peptide population against time, assuming a single exponential decay, as previously described in *ProteinTurnover* algorithm [33].

Protein turnover typically exhibits first-order kinetics, and the first-order rate constant (k) is related to the half-life of the particular peptide by the expression, $t_{1/2}=(\ln(2))/k$. In this study, the turnover rate was represented by the $\log_2 k$ values, which are more normally distributed than the untransformed rate constants. After obtaining the turnover results from *ProteinTurnover*, peptides were selected for subsequent inclusion in protein turnover calculations by applying the following filtering criteria: (1) the visual score of the spectral fitting (to the beta-binomial model) must be greater than 80; (2) the standard error of the turnover rate must be less than 10; and (3) data must be available for 3 or more time points. The $\log_2 k$ data of the selected and unique peptides were then averaged to obtain the protein turnover rate.

Estimating the Difference in $\log_2 k$ due to Heat Stress

The selected peptides were analyzed in R to calculate the difference in turnover rate between the control and treated groups. A linear mixed model (LMM) fit with restricted maximum likelihood (using the lme4 package) was applied to estimate the change of protein $\log_2 k$ between the control and heat-treated group based on peptide $\log_2 k$ data. The used formula is listed as follows:

$$\log_2 k \sim 0 + \text{ID} + \text{ID:temp} + (1|\text{Sequence:ID}),$$

where "ID" represents the protein UniProt accession number, "temp" represents either the control or 30°C group, and "Sequence" represents the peptide amino acid sequence. In the end, only proteins with significant changes in $\log_2 k$ (p-value less than 0.05) were included in Supplementary Table S-2. Only proteins with more than one computable unique peptide in both the control and heat-treated group were selected to generate histograms and box plots (Figure 5, 6 and 7).

5. Conclusions

This study provides a comprehensive overview of the dynamics of proteins in plants in response to moderate heat stress. Conducted at the cellular level, it involved the separation of soluble and membrane enrichments using ^{15}N-stable isotope labeling and the *ProteinTurnover* algorithm for automated data extraction and turnover rate calculation. A total of 571 proteins with significant changes in turnover rates were identified in response to elevated temperature in Arabidopsis seedling tissues. Root proteins involved in the redox signaling pathway, stress response, amino acid metabolism, GST metabolism, protein synthesis, protein degradation, and cellular organization exhibited less pronounced change in turnover to shoot proteins. Conversely, proteins involved in GST metabolism, photorespiration, protein folding, secondary metabolism, stress response, redox signaling pathway, and the beta-glucosidase family displayed the most notable alterations in turnover rates under elevated temperature conditions. Notably, proteins involved in major carbohydrate metabolism, glycolysis, protein synthesis, and mitochondrial ATP synthesis showed the smallest changes in turnover under this stress. This comprehensive study underscores the adaptive mechanisms of plants at the proteomic level in response to heat stress, offering insights for

 doi:10.20944/preprints202405.0780.v1

future agricultural strategies aimed at enhancing crop resilience and productivity in the context of global climate change.

Supplementary Materials: The following supporting information can be downloaded at the website of this paper posted on Preprints.org, Table S-1: Number of selected peptides after applying each sequential threshold rule and number of proteins identified with significant or insignificant changes in turnover rate after treatment with high temperature. Table S-2: List of proteins with significant changes in turnover rate (k) due to 30˚C treatment ($p < 0.05$) identified in the enriched soluble, organelle, and microsomal fractions of Arabidopsis root or shoot seedlings.

Author Contributions: Research and investigation, K.-T. F.; analysis and writing, K.-T. F and Y.X. All authors have read and agreed to the published version of the manuscript.

Funding: K.-T.F. and Y.X. acknowledge the NSF Plant Genome Research Program grants IOS-1238812 and IOS-1400818. Y.X. acknowledges the Office of Basic Energy Sciences at the U.S. Department of Energy Grants DE-FOA-0001650 and DE-FG02-91ER20021.

Data Availability Statement: The data presented in this study are available in Supplementary Materials.

Acknowledgments: K.-T.F and Y.X. acknowledge the support from Dr. Adrian D. Hegeman, Dr. William M. Gray, Dr. Jerry D. Cohen, and the support from the Department of Plant and Microbial Biology, the Department of Horticultural Science, the Microbial and Plant Genomics Institute, and Informatics Institute at the University of Minnesota. K.-T.F acknowledges the support of Dr. Yet-Ran Chen and the support of the Agricultural Biotechnology Research Center at Academia Sinica. Y.X. acknowledges the support of Dr. Thomas D. Sharkey and the support of MSU-DOE Plant Research Laboratory of Michigan State University.

Conflicts of Interest: The authors declare no conflict of interest.

References

1. Chaloner, T.M.; Gurr, S.J.; Bebber, D.P. Plant Pathogen Infection Risk Tracks Global Crop Yields under Climate Change. *Nat. Clim. Chang.* **2021**, *11*, 710–715.
2. Wing, I.S.; De Cian, E.; Mistry, M.N. Global Vulnerability of Crop Yields to Climate Change. *J. Environ. Econ. Manage.* **2021**, *109*, 102462.
3. *Genes for Plant Abiotic Stress*; Matthew A. Jenks, A.J.W., Ed.; Wiley-Blackwell: Oxford, UK, 2010; ISBN 9780813815022.
4. Xu, Y.; Fu, X. Reprogramming of Plant Central Metabolism in Response to Abiotic Stresses: A Metabolomics View. *Int. J. Mol. Sci.* **2022**, *23*, 5716.
5. Yeh, C.H.; Kaplinsky, N.J.; Hu, C.; Charng, Y.Y. Some like It Hot, Some like It Warm: Phenotyping to Explore Thermotolerance Diversity. *Plant Sci.* **2012**, *195*, 10–23, doi:10.1016/j.plantsci.2012.06.004.
6. Wahid, A.; Gelani, S.; Ashraf, M.; Foolad, M.R. Heat Tolerance in Plants: An Overview. *Environ. Exp. Bot.* **2007**, *61*, 199–223, doi:10.1016/j.envexpbot.2007.05.011.
7. Xu, Y.; Freund, D.M.; Hegeman, A.D.; Cohen, J.D. Metabolic Signatures of Arabidopsis Thaliana Abiotic Stress Responses Elucidate Patterns in Stress Priming, Acclimation, and Recovery. *Stress Biol.* **2022**, doi:10.1007/s44154-022-00034-5.
8. Crawford, A.J.; McLachlan, D.H.; Hetherington, A.M.; Franklin, K.A. High Temperature Exposure Increases Plant Cooling Capacity. *Curr. Biol.* **2012**, *22*, R396–R397.
9. Berry, J.; Bjorkman, O. Photosynthetic Response and Adaptation to Temperature in Higher Plants. *Annu. Rev. Plant Physiol.* **1980**, *31*, 491–543.
10. Yamane, Y.; Kashino, Y.; Koike, H.; Satoh, K. Effects of High Temperatures on the Photosynthetic Systems in Spinach: Oxygen-Evolving Activities, Fluorescence Characteristics and the Denaturation Process. *Photosynth. Res.* **1998**, *57*, 51–59.
11. Kurek, I.; Chang, T.K.; Bertain, S.M.; Madrigal, A.; Liu, L.; Lassner, M.W.; Zhu, G. Enhanced Thermostability of Arabidopsis Rubisco Activase Improves Photosynthesis and Growth Rates under Moderate Heat Stress. *Plant Cell* **2007**, *19*, 3230–3241.
12. Crafts-Brandner, S.J.; Salvucci, M.E. Rubisco Activase Constrains the Photosynthetic Potential of Leaves at High Temperature and CO2. *Proc. Natl. Acad. Sci. U. S. A.* **2000**, *97*, 13430–13435, doi:10.1073/pnas.230451497.
13. Ding, Y.; Shi, Y.; Yang, S. Molecular Regulation of Plant Responses to Environmental Temperatures. *Mol. Plant* **2020**, *13*, 544–564.
14. Qu, A.-L.; Ding, Y.-F.; Jiang, Q.; Zhu, C. Molecular Mechanisms of the Plant Heat Stress Response. *Biochem. Biophys. Res. Commun.* **2013**, *432*, 203–207.

15. Williams, B.; Kabbage, M.; Britt, R.; Dickman, M.B. AtBAG7, an Arabidopsis Bcl-2–Associated Athanogene, Resides in the Endoplasmic Reticulum and Is Involved in the Unfolded Protein Response. *Proc. Natl. Acad. Sci.* **2010**, *107*, 6088–6093.
16. Fields, P.A. Protein Function at Thermal Extremes: Balancing Stability and Flexibility. *Comp. Biochem. Physiol. Part A Mol. Integr. Physiol.* **2001**, *129*, 417–431.
17. Mittler, R. Oxidative Stress, Antioxidants and Stress Tolerance. *Trends Plant Sci.* 2002, *7*, 405–410.
18. Rizhsky, L.; Liang, H.; Shuman, J.; Shulaev, V.; Davletova, S.; Mittler, R. When Defense Pathways Collide. The Response of Arabidopsis to a Combination of Drought and Heat Stress. *Plant Physiol.* **2004**, *134*, 1683–1696.
19. Frank, G.; Pressman, E.; Ophir, R.; Althan, L.; Shaked, R.; Freedman, M.; Shen, S.; Firon, N. Transcriptional Profiling of Maturing Tomato (Solanum Lycopersicum L.) Microspores Reveals the Involvement of Heat Shock Proteins, ROS Scavengers, Hormones, and Sugars in the Heat Stress Response. *J. Exp. Bot.* **2009**, *60*, 3891–3908.
20. Yamakawa, H.; Hirose, T.; Kuroda, M.; Yamaguchi, T. Comprehensive Expression Profiling of Rice Grain Filling-Related Genes under High Temperature Using DNA Microarray. *Plant Physiol.* **2007**, *144*, 258–277.
21. Oshino, T.; Abiko, M.; Saito, R.; Ichiishi, E.; Endo, M.; Kawagishi-Kobayashi, M.; Higashitani, A. Premature Progression of Anther Early Developmental Programs Accompanied by Comprehensive Alterations in Transcription during High-Temperature Injury in Barley Plants. *Mol. Genet. Genomics* **2007**, *278*, 31–42.
22. Qin, D.; Wu, H.; Peng, H.; Yao, Y.; Ni, Z.; Li, Z.; Zhou, C.; Sun, Q. Heat Stress-Responsive Transcriptome Analysis in Heat Susceptible and Tolerant Wheat (Triticum Aestivum L.) by Using Wheat Genome Array. *BMC Genomics* **2008**, *9*, 1–19.
23. Fernandes, J.; Morrow, D.J.; Casati, P.; Walbot, V. Distinctive Transcriptome Responses to Adverse Environmental Conditions in Zea Mays L. *Plant Biotechnol. J.* **2008**, *6*, 782–798.
24. Yángüez, E.; Castro-Sanz, A.B.; Fernández-Bautista, N.; Oliveros, J.C.; Castellano, M.M.; Ferna, N.; Ya, E. Analysis of Genome-Wide Changes in the Translatome of Arabidopsis Seedlings Subjected to Heat Stress. *PLoS One* **2013**, *8*, e71425, doi:10.1371/journal.pone.0071425.
25. Lee, D.G.; Ahsan, N.; Lee, S.H.; Kyu, Y.K.; Jeong, D.B.; Lee, I.J.; Lee, B.H. A Proteomic Approach in Analyzing Heat-Responsive Proteins in Rice Leaves. *Proteomics* **2007**, *7*, 3369–3383, doi:10.1002/pmic.200700266.
26. Kosová, K.; Vítámvás, P.; Prášil, I.T.; Renaut, J. Plant Proteome Changes under Abiotic Stress—Contribution of Proteomics Studies to Understanding Plant Stress Response. *J. Proteomics* **2011**, *74*, 1301–1322.
27. Li, L.; Nelson, C.J.; Solheim, C.; Whelan, J.; Millar, A.H. Determining Degradation and Synthesis Rates of Arabidopsis Proteins Using the Kinetics of Progressive 15N Labeling of Two-Dimensional Gel-Separated Protein Spots. *Mol. Cell. Proteomics* **2012**, *11*.
28. Nelson, C.J.; Li, L.; Jacoby, R.P.; Millar, A.H. Degradation Rate of Mitochondrial Proteins in Arabidopsis Thaliana Cells. *J. Proteome Res.* **2013**, *12*, 3449–3459.
29. Sperling, E.; Bunner, A.E.; Sykes, M.T.; Williamson, J.R. Quantitative Analysis of Isotope Distributions in Proteomic Mass Spectrometry Using Least-Squares Fourier Transform Convolution. *Anal. Chem.* **2008**, *80*, 4906–4917.
30. Nelson, C.J.; Alexova, R.; Jacoby, R.P.; Harvey Millar, A. Proteins with High Turnover Rate in Barley Leaves Estimated by Proteome Analysis Combined with in Planta Isotope Labeling. *Plant Physiol.* **2014**, doi:10.1104/pp.114.243014.
31. Ishihara, H.; Obata, T.; Sulpice, R.; Fernie, A.R.; Stitt, M. Quantifying Protein Synthesis and Degradation in Arabidopsis by Dynamic 13CO2 Labeling and Analysis of Enrichment in Individual Amino Acids in Their Free Pools and in Protein. *Plant Physiol.* **2015**, *168*, 74–93.
32. Li, L.; Nelson, C.J.; Trösch, J.; Castleden, I.; Huang, S.; Millar, A.H. Protein Degradation Rate in Arabidopsis Thaliana Leaf Growth and Development. *Plant Cell* **2017**, doi:10.1105/tpc.16.00768.
33. Fan, K.T.; Rendahl, A.K.; Chen, W.P.; Freund, D.M.; Gray, W.M.; Cohen, J.D.; Hegeman, A.D. Proteome Scale-Protein Turnover Analysis Using High Resolution Mass Spectrometric Data from Stable-Isotope Labeled Plants. *J. Proteome Res.* **2016**, *15*, 851–867, doi:10.1021/acs.jproteome.5b00772.
34. Evans, E.M.; Freund, D.M.; Sondervan, V.M.; Cohen, J.D.; Hegeman, A.D. Metabolic Patterns in Spirodela Polyrhiza Revealed by 15N Stable Isotope Labeling of Amino Acids in Photoautotrophic, Heterotrophic, and Mixotrophic Growth Conditions. *Front. Chem.* **2018**, *6*, 191.
35. Hartigan, J.A.H. and P.M. The Dip Test of Unimodality. *Ann. Statis* **1985**, *13*, 70–84.
36. Brady T. West, Kathleen B. Welch, A.T.G. *Linear Mixed Models: A Practical Guide Using Statistical Software*; Chapman and Hall–CRC: Boca Raton, FL, 2007; ISBN 1-584-88480-0.
37. Kumar, S.V.; Wigge, P.A. H2A. Z-Containing Nucleosomes Mediate the Thermosensory Response in Arabidopsis. *Cell* **2010**, *140*, 136–147.
38. Xu, Q.; Huang, B. Growth and Physiological Responses of Creeping Bentgrass to Changes in Air and Soil Temperatures. *Crop Sci.* **2000**, *40*, 1363–1368.

39. Xu, Y.; Fu, X.; Sharkey, T.D.; Shachar-Hill, Y.; Walker, B.J. The Metabolic Origins of Non-Photorespiratory CO2 Release during Photosynthesis: A Metabolic Flux Analysis. *Plant Physiol.* **2021**, *186*, 297–314, doi:10.1093/plphys/kiab076.
40. Xu, Y.; Wieloch, T.; Kaste, J.A.M.; Shachar-Hill, Y.; Sharkey, T.D. Reimport of Carbon from Cytosolic and Vacuolar Sugar Pools into the Calvin–Benson Cycle Explains Photosynthesis Labeling Anomalies. *Proc. Natl. Acad. Sci.* **2022**, *119*, e2121531119.
41. Xu, Y.; Koroma, A.A.; Weise, S.E.; Fu, X.; Sharkey, T.D.; Shachar-Hill, Y. Daylength Variation Affects Growth, Photosynthesis, Leaf Metabolism, Partitioning, and Metabolic Fluxes. *Plant Physiol.* **2024**, *194*, 475–490.
42. Li, T.; Pang, N.; He, L.; Xu, Y.; Fu, X.; Tang, Y.; Shachar-Hill, Y.; Chen, S. Re-Programing Glucose Catabolism in the Microalga Chlorella Sorokiniana under Light Condition. *Biomolecules* **2022**, *12*, 939.
43. Fu, X.; Xu, Y. Dynamic Metabolic Changes in Arabidopsis Seedlings under Hypoxia Stress and Subsequent Reoxygenation Recovery. *Stresses* **2023**, *3*, 86–101.
44. Urano, K.; Kurihara, Y.; Seki, M.; Shinozaki, K. 'Omics' Analyses of Regulatory Networks in Plant Abiotic Stress Responses. *Curr. Opin. Plant Biol.* **2010**, *13*, 132–138.
45. Becker, J.; Craig, E. a Heat-Shock Proteins as Molecular Chaperones. *Eur. J. Biochem.* **1994**, *219*, 11–23.
46. Oh, S.E.; Yeung, C.; Babaei-Rad, R.; Zhao, R. Cosuppression of the Chloroplast Localized Molecular Chaperone HSP90. 5 Impairs Plant Development and Chloroplast Biogenesis in Arabidopsis. *BMC Res. Notes* **2014**, *7*, 1–15.
47. Mattoo, R.U.H.; Goloubinoff, P. Molecular Chaperones Are Nanomachines That Catalytically Unfold Misfolded and Alternatively Folded Proteins. *Cell. Mol. Life Sci.* **2014**, *71*, 3311–3325.
48. Suzuki, K.; Nakanishi, H.; Bower, J.; Yoder, D.W.; Osteryoung, K.W.; Miyagishima, S. Plastid Chaperonin Proteins Cpn60 Alpha and Cpn60 Beta Are Required for Plastid Division in Arabidopsis Thaliana. *BMC Plant Biol.* **2009**, *9*, 38, doi:10.1186/1471-2229-9-38.
49. Nash, D.; Miyao, M.; Murata, N. Heat Inactivation of Oxygen Evolution in Photosystem II Particles and Its Acceleration by Chloride Depletion and Exogenous Manganese. *Biochim. Biophys. Acta - Bioenerg.* **1985**, *807*, 127–133, doi:10.1016/0005-2728(85)90115-X.
50. Armond, P. a; Schreiber, U.; Björkman, O. Photosynthetic Acclimation to Temperature in the Desert Shrub, Larrea Divaricata: II. Light-Harvesting Efficiency and Electron Transport. *Plant Physiolgoy* **1978**, *61*, 411–415, doi:10.1104/pp.61.3.411.
51. Yamashita, T.; Butler, W.L. Inhibition of Chloroplasts by UV-Irradiation and Heat-Treatment. *Plant Physiolgoy* **1968**, *43*, 2037–2040, doi:10.1104/pp.43.12.2037.
52. Betterle, N.; Ballottari, M.; Hienerwadel, R.; Dall'Osto, L.; Bassi, R. Dynamics of Zeaxanthin Binding to the Photosystem II Monomeric Antenna Protein Lhcb6 (CP24) and Modulation of Its Photoprotection Properties. *Arch. Biochem. Biophys.* **2010**, *504*, 67–77.
53. Marutani, Y.; Yamauchi, Y.; Miyoshi, A.; Inoue, K.; Ikeda, K.; Mizutani, M.; Sugimoto, Y. Regulation of Photochemical Energy Transfer Accompanied by Structural Changes in Thylakoid Membranes of Heat-Stressed Wheat. *Int. J. Mol. Sci.* **2014**, *15*, 23042–23058.
54. Volkov, R.A.; Panchuk, I.I.; Mullineaux, P.M.; Schöffl, F. Heat Stress-Induced H 2 O 2 Is Required for Effective Expression of Heat Shock Genes in Arabidopsis. *Plant Mol. Biol.* **2006**, *61*, 733–746.
55. Zimmermann, P.; Hirsch-Hoffmann, M.; Hennig, L.; Gruissem, W. GENEVESTIGATOR. Arabidopsis Microarray Database and Analysis Toolbox. *Plant Physiolgoy* **2004**, *136*, 2621–2632, doi:10.1104/pp.104.046367.
56. Pnueli, L.; Liang, H.; Rozenberg, M.; Mittler, R. Growth Suppression, Altered Stomatal Responses, and Augmented Induction of Heat Shock Proteins in Cytosolic Ascorbate Peroxidase (Apx1)-deficient Arabidopsis Plants. *Plant J.* **2003**, *34*, 187–203.
57. Correa-Aragunde, N.; Foresi, N.; Delledonne, M.; Lamattina, L. Auxin Induces Redox Regulation of Ascorbate Peroxidase 1 Activity by S-Nitrosylation/Denitrosylation Balance Resulting in Changes of Root Growth Pattern in Arabidopsis. *J. Exp. Bot.* **2013**, *64*, 3339–3349.
58. Nagano, A.J.; Fukao, Y.; Fujiwara, M.; Nishimura, M.; Hara-Nishimura, I. Antagonistic Jacalin-Related Lectins Regulate the Size of ER Body-Type β-Glucosidase Complexes in Arabidopsis Thaliana. *Plant cell Physiol.* **2008**, *49*, 969–980.
59. Mayfield, J.D.; Folta, K.M.; Paul, A.-L.; Ferl, R.J. The 14-3-3 Proteins Mu and Upsilon Influence Transition to Flowering and Early Phytochrome Response. *Plant Physiolgoy* **2007**, *145*, 1692–1702, doi:10.1104/pp.107.108654.
60. Mayfield, J.D.; Paul, A.-L.; Ferl, R.J. The 14-3-3 Proteins of Arabidopsis Regulate Root Growth and Chloroplast Development as Components of the Photosensory System. *J. Exp. Bot.* **2012**, *63*, 3061–3070.
61. Gampala, S.S.; Kim, T.W.; He, J.X.; Tang, W.; Deng, Z.; Bai, M.Y.; Guan, S.; Lalonde, S.; Sun, Y.; Gendron, J.M.; et al. An Essential Role for 14-3-3 Proteins in Brassinosteroid Signal Transduction in Arabidopsis. *Dev. Cell* **2007**, *13*, 177–189, doi:10.1016/j.devcel.2007.06.009.

62. Usadel, B.; Poree, F.; Nagel, A.; Lohse, M.; Czedik-Eysenberg, A.; Stitt, M. A Guide to Using MapMan to Visualize and Compare Omics Data in Plants: A Case Study in the Crop Species, Maize. *Plant. Cell Environ.* **2009**, *32*, 1211–1229.
63. Yang, X.; Chen, W.; Rendahl, A.K.; Hegeman, A.D.; Gray, W.M.; Cohen, J.D. Measuring the Turnover Rates of Arabidopsis Proteins Using Deuterium Oxide: An Auxin Signaling Case Study. *Plant J.* **2010**, *63*, 680–695.
64. Sun, L.; Zhu, G.; Dovichi, N.J. Comparison of the LTQ-Orbitrap Velos and the Q-Exactive for Proteomic Analysis of 1-1000 Ng RAW 264.7 Cell Lysate Digests. *Rapid Commun. Mass Spectrom.* **2013**, *27*, 157–162, doi:10.1002/rcm.6437.
65. Chambers, M.C.; Maclean, B.; Burke, R.; Amodei, D.; Ruderman, D.L.; Neumann, S.; Gatto, L.; Fischer, B.; Pratt, B.; Egertson, J.; et al. A Cross-Platform Toolkit for Mass Spectrometry and Proteomics. *Nat. Biotechnol.* **2012**, *30*, 918–920, doi:10.1038/nbt.2377.
66. Geer, L.Y.; Markey, S.P.; Kowalak, J. a; Wagner, L.; Xu, M.; Maynard, D.M.; Yang, X.; Shi, W.; Bryant, S.H. Open Mass Spectrometry Search Algorithm. *J. Proteome Res.* **2004**, *3*, 958–964, doi:10.1021/pr0499491.
67. Searle, B.C. Scaffold: A Bioinformatic Tool for Validating MS/MS-Based Proteomic Studies. *Proteomics* **2010**, *10*, 1265–1269, doi:10.1002/pmic.200900437.
68. Giardine, B.; Riemer, C.; Hardison, R.C.; Burhans, R.; Elnitski, L.; Shah, P.; Zhang, Y.; Blankenberg, D.; Albert, I.; Taylor, J.; et al. Galaxy: A Platform for Interactive Large-Scale Genome Analysis. *Genome Res.* **2005**, *15*, 1451–1455, doi:10.1101/gr.4086505.
69. Blankenberg, D.; Kuster, G. Von; Coraor, N.; Ananda, G.; Lazarus, R.; Mangan, M.; Nekrutenko, A.; Taylor, J. Galaxy: A Web-Based Genome Analysis Tool for Experimentalists. *Curr. Protoc. Mol. Biol.* **2010**, 1–21, doi:10.1002/0471142727.mb1910s89.
70. Goecks, J.; Nekrutenko, A.; Taylor, J. Galaxy: A Comprehensive Approach for Supporting Accessible, Reproducible, and Transparent Computational Research in the Life Sciences. *Genome Biol.* **2010**, *11*, R86, doi:10.1186/gb-2010-11-8-r86.